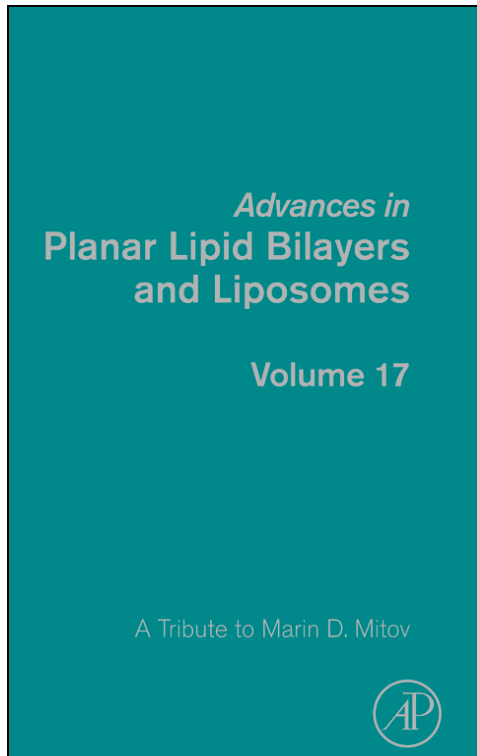


**Provided for non-commercial research and educational use only.  
Not for reproduction, distribution or commercial use.**

This chapter was originally published in the book *Advances in Planar Lipid Bilayers and Liposomes, Vol.17*, published by Elsevier, and the attached copy is provided by Elsevier for the author's benefit and for the benefit of the author's institution, for non-commercial research and educational use including without limitation use in instruction at your institution, sending it to specific colleagues who know you, and providing a copy to your institution's administrator.



All other uses, reproduction and distribution, including without limitation commercial reprints, selling or licensing copies or access, or posting on open internet sites, your personal or institution's website or repository, are prohibited. For exceptions, permission may be sought for such use through Elsevier's permissions site at:

<http://www.elsevier.com/locate/permissionusematerial>

From: Galya Staneva, Albena Momchilova, Kamen Koumanov and Miglena I. Angelova, *Developing Cell-Scale Biomimetic Systems: A Tool for Understanding Membrane Organization and Its Implication in Membrane-Associated Pathological Processes*. In Aleš Iglič and Julia Genova, editors: *Advances in Planar Lipid Bilayers and Liposomes, Vol.17*, Burlington: Academic Press, 2013, pp. 167-213.  
ISBN: 978-0-12-411516-3  
© Copyright 2013 Elsevier Inc.  
Academic Press



# Developing Cell-Scale Biomimetic Systems: A Tool for Understanding Membrane Organization and Its Implication in Membrane-Associated Pathological Processes

Galya Staneva<sup>\*</sup>, Albena Momchilova<sup>\*</sup>, Kamen Koumanov<sup>\*</sup>,  
Miglena I. Angelova<sup>†,‡,1</sup>

<sup>\*</sup>Institute of Biophysics and Biomedical Engineering, Bulgarian Academy of Sciences, Sofia, Bulgaria

<sup>†</sup>Physics Department, UPMC Université Paris 6, UFR 925, Paris, France

<sup>‡</sup>Matiere et Systèmes Complexes, UMR 7057, Université Paris-Diderot & CNRS, Paris, France

<sup>1</sup>Corresponding author: e-mail address: miglena.angelova@upmc.fr

## Contents

1. Concept of Membrane Rafts and Their Cellular Functions	168
2. Cell-Scale Biomimetic Systems as a Tool to Study Membrane Organization and Functioning	171
3. Effect of Sphingolipids on the Formation of Membrane Domains and Their Morphology in Biomimetic Systems	174
3.1 Sphingolipid structure	174
3.2 Role of Sphingolipids in membrane organization and function	175
3.3 Role of Sphingolipids in regulating raft-like domain formation in complex biomimetic systems	176
4. Visualization of Enzyme Activity in Biomimetic Systems	184
4.1 Sphingomyelinases	184
4.2 Phospholipases A2	189
5. Conclusions and Biological Implications	204
Acknowledgments	207
References	207

## Abstract

Giant unilamellar vesicles have become a versatile tool to mimic lateral membrane organization and membrane-associated processes in cells. The interest in sphingolipids has grown rapidly since the establishment of their role in cell signaling. This review summarizes our results on the impact of sphingolipids (sphingomyelin (SM), ceramide (CER), and sphingosine (SPH)) on the formation of membrane domains. CER and SPH form gel domains in the glycerophospholipid (GPL) matrix. Addition of CER and SPH to raft

mixtures induces larger liquid-ordered ( $L_o$ ) domains compared to the control phosphatidylcholine (PC)/SM/cholesterol (CHOL) ones. The presence of SM in PC/SM/CER/CHOL mixtures stabilizes the gel phase and thus decreases CER miscibility. More competitive CER/SM interactions compared to SM/CHOL ones change the conditions of  $L_o$  phase formation. The bacterial sphingomyelinase and secretory phospholipase A2 (sPLA2) activities on homogeneous and  $L_o/L_d$  (liquid-disordered) heterogeneous membranes were visualized. The enzyme-induced generation of CER from raft-containing SM leads to disintegration of the rafts. sPLA2 activity on substrate vesicles provokes vesicle shrinking and burst. SM is a sPLA2 inhibitor and its addition to the substrate vesicles increases the membrane resistance. CHOL restores sPLA2 activity in raft-containing mixtures. The enzyme induces continuous  $L_o$  domain budding and fission. CER augments, additionally, sPLA2 activity, and an appearance of holes in the membrane bilayer is observed. CER and CHOL seem to sequester SM making the phospholipid substrate more susceptible to enzyme attack. Possible molecular mechanism for  $L_o$  domain budding and fission is proposed, suggesting that PLA2 might be a factor for triggering, developing, and finalizing the process of rafts-transporting vesicle formation.



## 1. CONCEPT OF MEMBRANE RAFTS AND THEIR CELLULAR FUNCTIONS

The fluid mosaic model, proposed by Singer and Nicholson, states that most membrane constituents diffuse rapidly and randomly about the two-dimensional surface of the lipid bilayer [1]. Live cell imaging methods such as single particle tracking have provided considerable evidence that many receptors and even lipids are restricted in lateral mobility. These experimental observations, together with biochemical methods, established a compartmentalized conception of the cell plasma membrane. Three hypotheses of microdomain organization are discussed: membrane rafts [2], protein islands [3], and actin corals [4]. Simons and Gerl [5] revitalized membrane raft definition as dynamic, nanoscale, sterol-sphingolipid (SL)-enriched, ordered assemblies of proteins and lipids, in which the metastable raft resting state can be stimulated to coalesce into larger, more stable raft domains by specific lipid-lipid, protein-lipid, and protein-protein oligomerizing interactions. Thus, the dynamics of raft lipids and proteins must be considered as more relevant characteristics of the domains than their size.

Currently, lipid rafts have been implicated in a plethora of both physiological and pathological processes [6]. Besides the high content of SLs and cholesterol (CHOL), the membrane rafts contain saturated phosphatidylcholines (PCs), as well as small amounts of phosphatidylethanolamines and phosphatidylserines. The SLs ganglioside 1 and 2 (GM1 and GM2) are main

components of these assemblies and are commonly used as raft marker lipids. Fluorophores conjugated to cholera-toxin B subunit, which binds to the raft constituent ganglioside (GM) is extensively used to visualize rafts.

Rafts are postulated to be platforms that directly participate in the lateral recruitment of certain types of proteins, while trafficking through the Golgi as well as in the association of proteins with GPI anchors to non-clathrin-coated plasma membrane invaginations called caveolae [7]. The most widely studied function of rafts is to provide a distinct environment for signaling molecules, receptors, channels, recognition molecules, coupling factors, and enzymes. Receptors such as members of the tyrosine kinase Src family, G-proteins, and various receptor proteins like the platelet receptor P2X allow a specific regulation of pathways related to these molecules in the plasma membrane.

A role for lipid rafts in the transport of substrates, such as glucose and fatty acids into the cell, has been recently reported [8,9]. At present, there is evidence that at least a subset of plasma membrane insulin receptors reside in membrane rafts/caveolae. Furthermore, molecular components of insulin signaling also reside in or are recruited into these structures, and this recruitment is required for at least some insulin actions in adipocytes (insulin-stimulated glucose transport) [8].

Adipocytes are the primary site for lipid storage and mobilization and, as such, one of their major roles is the uptake and release of long-chain fatty acids (LCFAs). Several proteins in the adipocyte plasma membrane have been implicated in fatty acid transport or binding, such as plasma membrane fatty acid-binding protein, fatty acid transport protein, caveolin-1, and fatty acid translocase (FAT/CD36). Recently, it has been shown that at the cell surface FAT/CD36 is exclusively located within lipid rafts, whereas intracellularly FAT/CD36 is found in nonlipid raft membranes cofractionating with the Golgi apparatus [9]. Thus, lipid raft microdomains might control fatty acid uptake by regulating FAT/CD36 surface availability. Caveolin-1 might target FAT/CD36 to the plasma membrane. However, the mechanism of action and regulation of FAT/CD36, as well as the other proteins involved in LCFA uptake, is not well understood and is the subject of ongoing investigations by a number of groups.

Among other beneficial processes are axonal growth and branching [10] and the stabilization of synapses [11]. During development, axons elongate and reach their appropriate targets to form neuronal networks. The tip of an elongating axon, called the growth cone, explores its surrounding extracellular environment and migrates toward its target, pulling the axon behind it. It has been suggested that lipid rafts serve as a platform for localized signaling

during growth cone migration and turning [10]. Upon encountering molecular cues in the extracellular environment, plasma membrane rafts recruit cytoplasmic key components that reorganize the cytoskeleton and regulate cell adhesion molecule trafficking. Lipid rafts should be heterogeneous entities recruiting diverse sets of functional molecules to different subcellular regions, thereby generating region-specific signals in the growth cone. Such polarity generated by raft-dependent signaling plays a central role in axon growth and guidance. However, intracellular signaling initiators recruited to raft membranes after the growth cone encounters an extracellular cue remain to be identified, and the mechanisms for activating, amplifying, and localizing their downstream components are also largely unknown. The main challenges for the future include the identification of compositional and structural diversity in raft populations and the characterization of corresponding raft-dependent signals that ultimately converge on the cytoskeletal and adhesion machinery [6,10].

A number of proteins involved in apoptotic signals have been located in lipid rafts [12–14]. Programmed cell death or apoptosis is a genetically regulated process conserved throughout the evolution. Apoptosis allows removal of abnormal growing cells and controls homeostasis. Apoptosis eliminates cells in an ordered manner and deregulation of the apoptotic machinery can lead to many diverse diseases. Irreversible loss of cells in the brain and heart can have dramatic consequences for the organism, whereas potentially dangerous cells, which show resistance to apoptotic responses, are thought to be the origin of many types of cancer. Deregulation in the suicide program has been experimentally demonstrated in Alzheimer, Parkinson, autoimmunity, cancer, heart failure, HIV, inflammation, and osteoporosis [15,16]. Type I apoptosis is characterized by an extrinsic receptor-dependent pathway and requires the binding of a ligand to death receptors, such as Fas (CD95) or tumor necrosis factor, whereas type II apoptosis is an intrinsic pathway that involves cell organelles such as mitochondria or the endoplasmic reticulum. Both pathways share downstream cascades involving caspases, proteolytic, and lyolytic enzymes that initiate and execute apoptotic cell death.

Rafts can serve as a means of performing some therapeutic tasks. Fas-mediated apoptosis involves translocation of Fas—and downstream signaling molecules—into lipid rafts, a process that can be pharmacologically modulated [17,18]. FasL-independent clustering of Fas in membrane rafts generates high local concentrations of death receptor providing scaffolds for coupling adaptor and effector proteins involved in Fas-mediated apoptosis. Thus, lipid rafts act as the key point from which a potent death signal is

launched, becoming a new promising anticancer target. These findings set a novel framework for the development of more targeted therapies leading to intracellular Fas activation and recruitment of downstream signaling molecules into Fas-enriched lipid rafts.

Briefly, the importance of lipid raft signaling in the pathogenesis of a variety of conditions, such as neurodegenerative, cardiovascular and prion diseases, cancer, and HIV, has been elucidated over the recent years and makes these specific membrane domains an interesting target for pharmacological approaches in the prevention and cure of these diseases.



## **2. CELL-SCALE BIOMIMETIC SYSTEMS AS A TOOL TO STUDY MEMBRANE ORGANIZATION AND FUNCTIONING**

The biomimetic systems allow us to design appropriate studies of cellular membranes to answer important questions about their structure, properties, and functions. Curiosity to understand the fundamental basis of cell functioning gives us hope to discover the magic pill against any disease. It drives scientists from all over the world to create more and more sophisticated model systems in order to be able to give simple answers to the complex problems of cellular life. Thus, many generations of scientists will become architects of the future artificial cell without aiming at that.

During the past decades, giant unilamellar vesicles (GUVs) have become an extremely versatile tool to mimic lateral membrane organization in cells. However, the development of each model system goes hand in hand with advancements of the new technologies. Since the invention of the method of GUV electroformation by Angelova and coworkers at the end of the 1980s to the beginning of the 1990s [19,20], when the first GUV images were made by simple black and white photography, the technique has undergone a number of variations [21–23] and now GUVs are imaged by the last generation optical microscopes and CCD cameras. Giant vesicles are spherical free-standing bilayer assemblies with diameters of 10–100  $\mu\text{m}$ . Since GUVs equal or exceed cellular dimensions, they are microscopically visible and we can select and operate on one vesicle at a time. At first, significant information was obtained about the physical properties of bilayers and shape transformations of vesicles, and in this context, the pioneering studies by the groups of Evans [24], Sackmann [25], Needham [26], and Bothorel [27] should be mentioned.

Recently, modified GUV electroformation protocol focusing specifically on high-salinity conditions (up to 250 mM NaCl) was proposed by

Pott *et al.* [21]. High GUV electroformation rates have been attained in electrolyte-containing buffers at physiologically relevant concentrations. Thanks to this protocol, Montes *et al.* [28] were able to create the first GUV from native membranes using red blood cell ghosts as deposits. Thus, “the big hurdle in GUV production at physiological conditions,” according to Pott and colleagues [21], has been overcome, which should obviously widen the use of GUV for biochemical, biological, or biophysical studies. Earlier, successful formation of giant liposomes at high ionic strengths was reported but the inclusion of a charged lipid in the mixtures is required, such as phosphatidylglycerol, phosphatidylserine, phosphatidic acid, or cardiolipin [29].

Studies on the interaction of active macromolecules such as proteins, DNA, and enzymes with organized lipid interfaces are conducted using a variety of systems, including small (SUV) and large unilamellar vesicles (LUV), multilamellar vesicles, and monolayers at the air–water interface. Because of their particular characteristics (size and lamellarity), these model membranes are not necessarily accurate descriptions of cell membranes. It is noteworthy that in some techniques such as X-ray diffraction experiments, electron-spin resonance spectroscopy, and fluorescence spectroscopy, these model systems still remain the unique options to carry out precise measurements.

GUVs have a minimum curvature and mimic cell membrane in the best way compared to the above-mentioned models. They are ideal for studying lipid/lipid [30–35], lipid/DNA [36], and lipid/protein [37–42] interactions, and last, but not least, provide a view of an enzyme at work [43–47]. Lipid phase separation [23,48–51] and various morphological changes such as domain budding and fission [45,47,52], vesicle burst and shrinking [43], and “cytomimetic” processes [53] can be viewed and monitored as directly as they can by using living cells. GUVs have also been used to determine whether binding a motor protein to a lipid bilayer would be sufficient to generate membrane tubes [54].

One of the most important contributions of GUV experiments was based on the raft hypothesis that the formation of lipid domains enriched in (glyco) sphingolipids, CHOL, and saturated phospholipids can be driven by characteristic lipid–lipid interactions, suggesting that rafts ought to form in model membranes composed of appropriate lipids [5,7,31]. In fact, domains with raft-like properties (domains in liquid-ordered ( $L_o$ ) phase) were found to coexist with fluid lipid regions (liquid-disordered ( $L_d$ ) phase) in vesicles formed from equimolar mixtures of unsaturated phospholipid–CHOL–sphingomyelin (SM), and unsaturated phospholipid–CHOL–saturated PCs. Furthermore, it has

been a long-standing, open question whether a phase domain in one monolayer of the lipid bilayer is exactly superimposed with a corresponding domain of the same phase in the opposing monolayer. Detailed topology of coexisting phase domains over the surface of a vesicle demonstrates that they are exactly superimposed in opposing symmetric monolayers [51].

Another strong argument supporting the raft hypothesis is the observation of lipid-based phase separation into  $L_o$ - and  $L_d$ -like phases at first in natural lipids extracted from brush border membranes [31] in isolated giant plasma membrane vesicles formed by membrane blebbing [37] and in plasma membrane lipids extracted from fibroblasts cultured as two-dimensional monolayer and in tissue-like three-dimensional conditions [55].

Other contributions of GUV research related to the raft hypothesis were to provide rapid information about lipid mixing and to allow the direct visualization of the lipid phase separation that is not readily available from other methods. Complex and precise phase diagrams were constructed on the base of GUV composed of binary, ternary, and quaternary lipid mixtures [32,56–60]. It was also found that the molecular structure of a sterol determines its ability to induce raft-like domains [34,61,62]. Moreover, GM1, an essential raft component, hinders formation of large micron-scale  $L_o$  domains and it suggests that GM1 could “arrest”  $L_o$  domain growth through a decreasing effect of the line tension between  $L_o$  and  $L_d$  phases [30].

Undoubtedly, the formation of perfectly round-shaped domains, growing in size by fusion, is a manifestation of liquid–liquid immiscibility. Such raft-forming mixtures are characterized with miscibility transition points at which composition fluctuations arise over a wide range of time and length scales [63]. These miscibility transition points depend on the lipid composition and temperature. Nowadays, it is a challenge for interface scientists to seek biological agents (enzyme action, protein presence, and assemblies or creation of membrane and solute asymmetry) that can induce such miscibility transitions from two-phase coexisting regions to one phase and vice versa. An example of a similar process is the photoinduction of  $L_o$  microdomains caused by lipid chemical modifications [30,59,64].

All these outcomes demonstrate that GUV-containing  $L_o$  domains enriched in SLs and sterols, and coexisting with  $L_d$ , have become important tools for the modeling of properties and biological functions of membrane rafts. Although GUV  $L_o$  domains can only partially mimic the complex features of biological rafts (e.g., heterogeneity of composition, dynamic size distribution, recycling), these have been instrumental in evaluating current ideas as well as making new proposals for raft-associated mechanisms. The development of



more sophisticated cell-scale biomimetic systems together with high technologies would allow revealing the lipid/lipid, lipid/protein, and protein/protein communications in the lateral and transversal plane of cell membranes. Understanding of membrane functioning in health would ensure better control on the membrane-associated pathological processes.



### 3. EFFECT OF SPHINGOLIPIDS ON THE FORMATION OF MEMBRANE DOMAINS AND THEIR MORPHOLOGY IN BIOMIMETIC SYSTEMS

#### 3.1. Sphingolipid structure

SM and related molecules such as ceramide (CER) and sphingosine (SPH) make up the SL class of membrane lipids. The chemical structure of the SLs of particular interest in this chapter is summarized in Fig. 7.1. SM is composed of SPH, a fatty acid, a phosphate group and choline. CER and SPH are released by the sequential cleavage of SM. Phosphorylation of SPH leads

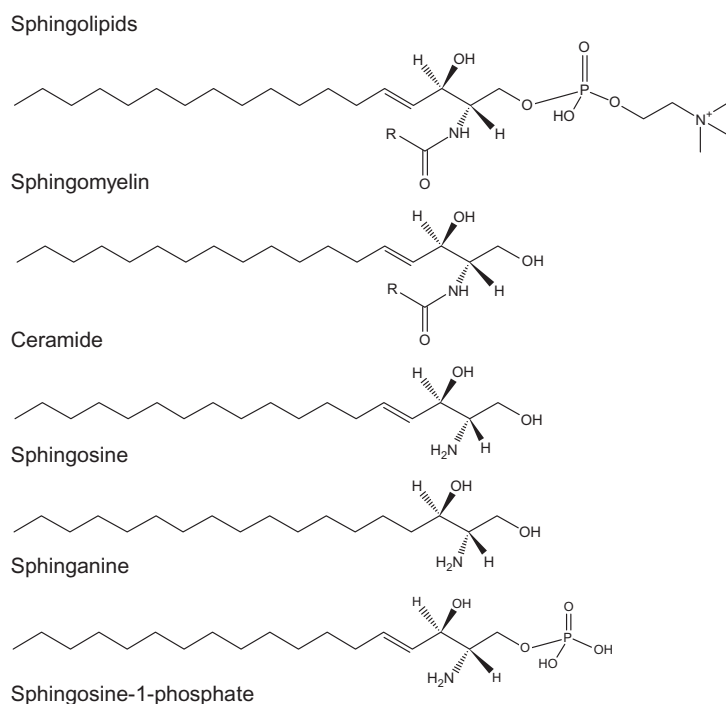


**Figure 7.1** Chemical structure of the sphingolipids: sphingomyelin, ceramide, sphingosine, sphinganine, and sphingosine-1-phosphate. Fatty acids in the lipids are designated as "R." Lipid structures were taken from the LIPID MAPS Lipidomics Gateway [65].

to the formation of sphingosine-1-phosphate (SPH-1-P). SPH is an 18-carbon amino alcohol with an unsaturated hydrocarbon chain. When the sphingoid base is acylated, the CER is formed. The amino group at the second carbon of the sphingoid base serves as the attachment site for the fatty acyl chain via an amide linkage. Typically, the acyl chains are long and saturated. Acyl chains of 18 carbons are common in bovine brain SM and GMs. GM is a molecule composed of a glycosphingolipid (CER and oligosaccharide) with one or more sialic acids linked on the sugar chain. Unsaturation in sphingolipid acyl chains is limited almost exclusively to single *cis* double bonds. High phase transition temperatures characteristic of SLs are due to the high degree of acyl chain saturation [66]. The presence of hydroxyl- and amido-groups confers on each molecule the ability to act simultaneously as hydrogen bond donor and acceptor [67]. Therefore, the SLs are able to form an intermolecular network of linkages that keeps them associated with each other. This feature is not shared by other membrane components such as GPLs, which can act only as hydrogen bond acceptors.

### 3.2. Role of Sphingolipids in membrane organization and function

The interest in SLs and their metabolites has grown very rapidly since the establishment of their important role in cell signaling. The mechanisms of action of CER and SPH-1-P have been particularly well studied. It is known that these two SLs exhibit opposite effects on various cellular processes such as apoptosis, cell differentiation, and growth. SPH-1-P exerts an inhibitory effect on apoptosis unlike CER, which stimulates this process [68,69]. The interest of many authors has been attracted by the so-called CER/SPH-1-P rheostat, that is, the ratio between these two lipids could determine the fate of a cell—apoptosis in case of high CER levels or cell survival if SPH-1-P predominates [70]. However, the intermediate product in the metabolic chain “CER/SPH-1-P,” SPH, has received less attention. Studies related to its mechanism of action are quite incomplete, although its essential role in the functioning of the “CER/SPH-1-P rheostat” is more than obvious.

Cell CER is either synthesized *de novo* [71] or originates as a product of the hydrolysis of SM by sphingomyelinase (SMase) [72] (Fig. 7.2). Membrane-bound SMases have been reported to be localized predominantly in membrane raft domains [73], implying that CER that is produced by the action of SMases is formed from substrate present in these domains [74]. It is assumed that cellular SPH is formed exclusively as a result of CER degradation, whereas its eventual *de novo* synthesis does not occur

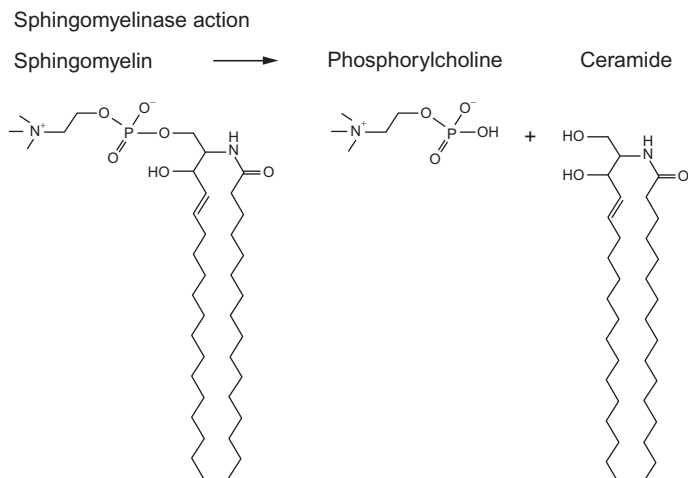


**Figure 7.2** Sphingomyelinase catalyzes the hydrolysis of sphingomyelin to produce phosphorylcholine and ceramide. *Lipid structures were taken from the LIPID MAPS Lipidomics Gateway [65].*

[75]. SPH generated by neutral ceramidase could also be found in the plasma membrane outer monolayer. This indicates that neutral ceramidase can actively participate in CER metabolism at plasma membrane level and thus be a mediator in the production of SPH-1-P [76]. According to some authors, the presence of acid SMases and neutral ceramidases at the cellular surface suggests that membrane rafts are the site for generation of SPH [77,78]. It has been demonstrated that endogenous human sphingosine kinase 1, and its substrate, D-erythro-sphingosine reside in the plasma membrane lipid raft domains [79]. These facts support the key role of CER and SPH in the SM signaling pathway and the importance of plasma membrane lipid microdomains in the performance of these processes.

### 3.3. Role of Sphingolipids in regulating raft-like domain formation in complex biomimetic systems

Although the studies addressing the role of SLs in cell death are numerous, many of the specific functions that these mediators regulate are still elusive [69]. The evidence implicating CER and SPH in cell death, sphingosine kinase 1, and SPH-1-P in cell survival is consistent, yet there appear to be differences in the mechanisms of cell signaling in different cell types as well as the signals generated by different stimuli. This suggests a versatile role for these lipids in cell function that can potentially be tailored for a therapeutic advantage.

That is why our studies have been devoted to the effect of CER and SPH on the lipid organization in membranes [80–82]. Special attention has been paid to the formation of membrane domains and their morphology in various lipid matrixes. We engineered complex GUVs comprising different ratios of naturally-occurring lipids such as egg-yolk PC, egg-yolk SM, egg-yolk CER, bovine brain SPH, and CHOL. Different patterns of domain formation in the micron scale were visualized using fluorescence microscopy in PC/CER and PC/SPH binary mixtures; PC/SM/CHOL, PC/CER/CHOL, and PC/SPH/CHOL ternary mixtures; and PC/CER/SM/CHOL and PC/SPH/SM/CHOL quaternary ones. We were able to determine the temperature of micron-scale domain formation (Table 7.1) and identify domain shape and size, as well as their dynamics.

Micron-scale miscibility transition temperatures ( $T_m$ ) were recorded as the temperatures at which visible domains appeared and then disappeared as temperature was decreased and then increased. This is described in detail by Veatch and Keller [32]. Transition temperature was defined as the average

**Table 7.1** Micron-scale miscibility transition temperature for different series of lipid mixtures composed of the following lipids: egg-yolk phosphatidylcholine (PC), egg-yolk sphingomyelin (SM), egg-yolk ceramide (CER), bovine brain sphingosine (SPH), and cholesterol (CHOL)

Lipid mixture	$T_{\text{micron-scale miscibility transition temperature}}$
<b>Binary mixtures</b>	
(PC/CER)	$L_{\beta}/L_d$
90/10	$(25.7 \pm 2.8) ^\circ\text{C}$
80/20	$(30.4 \pm 3.6) ^\circ\text{C}$
(PC/SPH)	
90/10	$(10.1 \pm 2.3) ^\circ\text{C}$
80/20	$(13.9 \pm 2.9) ^\circ\text{C}$
60/40	$(18.4 \pm 4.1) ^\circ\text{C}$
<b>Ternary mixtures</b>	
(PC/CER/CHOL)	$L_{\beta}/L_d$
80/10/10	$(25.4 \pm 2.2) ^\circ\text{C}$
70/10/20	$(17.2 \pm 3.3) ^\circ\text{C}$
60/10/30	$(4.5 \pm 4.4) ^\circ\text{C}$

*Continued*

**Table 7.1** Micron-scale miscibility transition temperature for different series of lipid mixtures composed of the following lipids: egg-yolk phosphatidylcholine (PC), egg-yolk sphingomyelin (SM), egg-yolk ceramide (CER), bovine brain sphingosine (SPH), and cholesterol (CHOL)—cont'd

Lipid mixture	$T_{\text{micron-scale miscibility transition temperature}}$
<b>(PC/SPH/CHOL)</b>	
70/20/10	$(14.2 \pm 3.1) ^\circ\text{C}$
60/20/20	$(10.2 \pm 2.9) ^\circ\text{C}$
50/20/30	$(5.8 \pm 2.2) ^\circ\text{C}$
<b>Control mixtures</b>	
<b>(PC/SM/CHOL)</b>	
	$L_o/L_d$
65/17.5/17.5	$(21.8 \pm 2.6) ^\circ\text{C}$
60/22.5/17.5	$(22.9 \pm 3.4) ^\circ\text{C}$
50/30/20	$(23.8 \pm 4.6) ^\circ\text{C}$
30/50/20	$(37.3 \pm 2.9) ^\circ\text{C}$
<b>Quaternary mixtures</b>	
<b>(PC/CER/SM/CHOL)</b>	
70/10/10/10	$(25.7 \pm 3.7) ^\circ\text{C}$ ( $L_\beta/L_d$ )
60/10/20/10	$(27.4 \pm 3.9) ^\circ\text{C}$ ( $L_\beta/L_d$ ); $(4.4 \pm 3.1) ^\circ\text{C}$ ( $L_o/L_d$ )
50/10/30/10	$(29.6 \pm 4.4) ^\circ\text{C}$ $L_d/L_\beta$
<b>(PC/CER/SM/CHOL)</b>	
55/10/17.5/17.5	$(33.6 \pm 2.7) ^\circ\text{C}$ ( $L_o/L_d$ )
50/15/17.5/17.5	$(36.3 \pm 3.1) ^\circ\text{C}$ ( $L_\beta/L_d$ ); $(17.4 \pm 3.5) ^\circ\text{C}$ ( $L_o/L_d$ )
45/20/17.5/17.5	$(10 \pm 4.4) ^\circ\text{C}$ (percolation $L_d/L_o$ ); $(4.2 \pm 3.9) ^\circ\text{C}$ $L_d/L_o/L_\beta$
<b>PC/SPH/SM/CHOL</b>	
50/20/10/20	$(17.9 \pm 3.4) ^\circ\text{C}$ ( $L_\beta/L_d$ ); $(9.8 \pm 3.9) ^\circ\text{C}$ ( $L_o/L_d$ )
40/20/20/20	$(25.7 \pm 4.3) ^\circ\text{C}$
30/20/30/20	$(37.2 \pm 2.4) ^\circ\text{C}$

$L_\beta$ , gel phase;  $L_d$ , liquid-disordered phase;  $L_o$ , liquid-ordered phase. The table summarizes the results published in Ref. [80,82].

of these two points. Standard deviations (SD) correspond to the averaged data from at least 10 vesicles. All vesicles were electroformed at 45 °C at which a high yield of vesicles was consistently obtained. The GUVs composed of the indicated mixtures were formed at higher temperatures but a difference in  $T_m$  greater than SD was not observed. In general, it should be noted that if the temperature of GUV formation is not higher than the temperature of ideal lipid miscibility, a variation in vesicle composition would be assumed.

Due to its relatively high melting point compared to the unsaturated GPLs, sphingolipids (SPH (Fig. 7.3), CER (Fig. 7.4), and SM (data are not shown)) were partially immiscible in the GPL matrix (Table 7.1) [80,82]. CER forms larger leaf-like domains compared to SPH [80,82]. Despite the structural differences in the polar headgroup (phosphocholine in SM and a single hydroxyl group in CER and SPH), these SLs form leaf-like gel domains. Such lipid segregation in membranes is possibly imposed by the hydrophobic mismatch between GPLs and SLs. The leaf-like structure of SL domains is maintained by the strong van der Waals interactions between the saturated hydrocarbon chains and the electrostatic repulsion between the lipid dipoles (or between the net positive charges

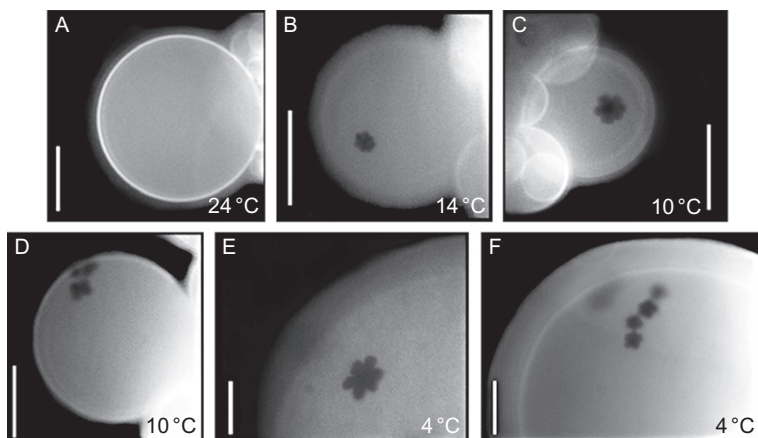


**Figure 7.3** Visualization of  $L_{\beta}/L_d$  phase separation in sphingosine-containing GUVs on the micron scale. PC/SPH 80/20 binary mixture yielded homogeneous vesicles in the temperature range from 37 to 15 °C (A). Domain formation at 14 °C (B). Well-resolved dark leaf-like domains at 10 °C (C). Clustering of small leaf-like domains at 10 °C (D). Formation of well-resolved petals at 4 °C (E). Assembly of two (D) and four (F) domains into clusters at 4 °C. The headgroup-labeled lipid analogue  $L\text{-}\alpha$ -phosphatidylethanolamine- $N$ -(lissamine rhodamine B sulfonyl) was used to visualize the phase coexistence. The marker is excluded from the more ordered phase and partitions predominantly in the disordered one. Bar 20  $\mu\text{m}$ . Reprinted from Ref. [82] with permission from Elsevier.

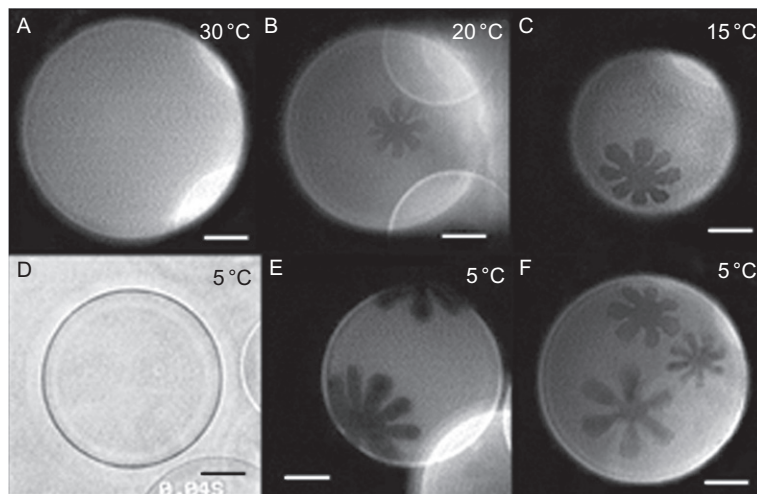


**Figure 7.4**  $L_{\beta}/L_d$  phase separation in PC/CER/CHOL 80/10/10 ternary mixture. Formation of leaf-like domains at about 25 °C (A and B) and their growth in size (B and C). The phase contrast observation shows no outward or inward budding of domain location (D). A larger number of domains are seen at low temperatures (E and F). The petals are characterized by a more elongated shape and finer attachment to the central area of the domains (F) compared to the PC/CER 80/20 binary mixture. CER formed larger leaf-like domains compared to SPH (Fig. 7.3). The fluorescent lipid analogue acyl 12:0 NBD PC (1-acyl-2-{12-[(7-nitro-2-1,3-benzoxadiazol-4-yl)amino]dodecanoyl}-sn-glycero-3-phosphocholine) was used to visualize the phase coexistence. Bar 20  $\mu\text{m}$ . Reprinted from Ref. [80] with permission from Elsevier.

of SPH molecules) [83,84]. Because SPH differs in structure from SM and CER (a small polar head, a single OH group, only one hydrocarbon chain, and the presence of a net positive charge), it is surprising that this molecule can form stable leaf-like domains like the other two-chain saturated lipids. Obviously, the high degree of hydrophobicity, based on the saturation of the fatty acid chains, is a unifying factor which determines the lipid phase behavior of the gel/liquid state.

The addition of CHOL to PC/SLs mixtures resulted in melting of the SL gel domains [80,82]. Each 10 mol% CHOL decreased the temperature of domain formation by about 8 °C in PC/CER binary mixtures (Table 7.1). Such an influence, but to a much lesser extent, is exerted by CHOL on SPH gel domains reducing the temperature of their formation by about 4 °C [80,81]. CHOL effect on the melting temperature of both SLs (CER and SPH) is fundamentally different from its effect on SM gel domains. The progressive enrichment of a PC/SM binary mixture with CHOL turned the gel/liquid phase coexistence into two partially

immiscible liquid phases, the  $L_o$  and  $L_d$  phases [32]. The high affinity of CHOL for phosphocholine-containing species, such as SM and saturated PC, and their specific interactions is a key factor for the formation of  $L_o$  phase. However, the mechanism of CHOL effect on the structurally identical hydrophobic parts of SM, CER, and SPH is different and the possible reason is apparently the lack of a phosphocholine polar headgroup in CER and SPH molecules. CHOL and CER in GPL matrix did not form  $L_o$  phase [80], neither did CHOL and SPH [82]. The formation of  $L_o$  phase in PC/SM/CHOL ternary mixtures and its visualization on the micron scale is a feature of the direct SM–CHOL interactions. The possible mechanism of melting of the other two SLs, CER and SPH, by CHOL, seems rather indirect [81]. The presence of CHOL resulted in an increase of the molecular order parameter of the  $L_d$  phase, which in turn increased the miscibility of these two SLs for disordered phase. Thus, the fraction of gel domains gradually decreased with the increase of CHOL content [80,82].

A specific interaction between SPH and CHOL, leading to the formation of condensed lipid complexes, has been reported [85]. The authors suggested that SPH had a similar behavior in terms of SM interaction with CHOL. However, the visualization of the domain pattern in PC/SPH/CHOL and PC/CER/CHOL ternary mixtures (leaf-like shape) compared to PC/SM/CHOL (round shape) showed radically different phase morphologies.

Further complication of the model system by the addition of SM to the ternary PC/CER/CHOL and PC/SPH/CHOL mixtures demonstrated the competition between CER and SM (or SPH and SM) for the interaction with CHOL.

In the series of quaternary mixtures, the impact of CER and SPH on the formation of micron-scale  $L_o$  phase has been examined. The addition of 10 mol % CER to PC/CER/SM/CHOL quaternary mixtures (50/10/20/20) did not interfere with the formation of  $L_o$  domains, that is, the properties of a liquid phase were governing [80]. However, larger CER proportions (20 and 30 mol%) led to the formation of gel domains at higher temperatures compared to PC/CER/CHOL 80/10/20 and PC/CER 90/10 control mixtures, and the formation of  $L_o$  domains was shifted to lower temperatures compared to raft-forming PC/SM/CHOL (60/20/20) mixture. Thus, we demonstrated that CER competed with CHOL for SM and formed more stable SM/CER gel domains leaving less available SM for the formation of  $L_o$  phase. The idea of competition between CHOL and CER was not a new one and was proposed for the first time by Megha and London [86]. Later, using atomic force microscopy, other authors reported that the addition of CER to raft



mixtures led to the formation of a third phase, thicker than the other two phases ( $L_o$  and  $L_d$ ) [87]. The formation of a third phase, obviously enriched in CER, within the  $L_o$  domains, is energetically beneficial, as the hydrophobic mismatch between the different phases is minimized. The effect of SPH on the fluid properties of  $L_o$  domains was similar to that of CER (10 mol%), but at twice as large concentrations (20 mol%) [80,82]. We found that SPH also enlarged the  $L_o$  phase fraction, but the question of whether it participated in the form of a gel within the  $L_o$  domains or as a homogeneous component of this phase, similar to SM, remained unsolved. The competition between SPH and CHOL for interaction with SM occurred in proportions in which  $SM < SPH$  (Fig. 7.5). The properties of the  $L_o$  phase were preponderant when  $SM \geq SPH$  (Fig. 7.6) unlike CER effect (PC/CER/SM/CHOL 40/20/20/20) (Fig. 7.7), where the temperatures of gel domain formation and  $L_o$  were well distinguished [80].

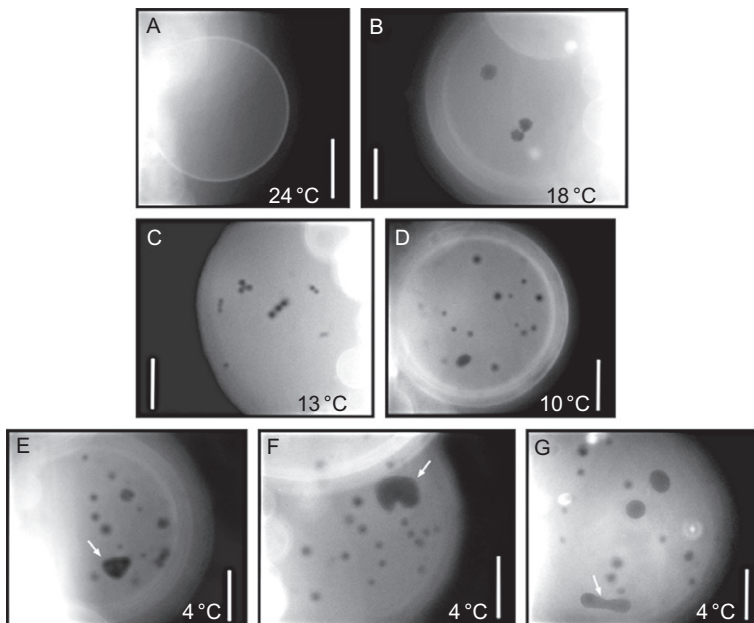


**Figure 7.5** Visualization of phase separation in a PC/SPH/SM/CHOL 50/20/10/20 quaternary mixture. Vesicles exhibited a homogenous appearance from 37 to 19 °C (A). Formation of  $L_\beta$  domains at 18 °C (B). Clusters of two or three  $L_\beta$  domains (C). Formation of  $L_o$  domains at 10 °C (D) and their increase in size by fusion (E–G). The headgroup-labeled lipid analogue  $L\text{-}\alpha$ -phosphatidylethanolamine- $N$ -(lissamine rhodamine B sulfonyl) was used to visualize the phase coexistence. Bar 20  $\mu\text{m}$ . Reprinted from Ref. [82] with permission from Elsevier.

Alanko *et al.* [88] showed that neither SPH nor sphinganine (Fig. 7.1) was able to displace CHOL from SM/CHOL domains, but the SPH/SM/CHOL ratio in their mixtures was 15/30/9, where the content of SM was more than twice that of SPH. This lipid ratio corresponds rather to SPH/SM/CHOL 20/20/20 and 20/30/20 in our experiments, where  $SM \geq SPH$ . In these cases, only  $L_o/L_d$  phase coexistence was observed and  $L_o$  domains formed at higher temperatures. Thus, from this line of argument, it can be concluded that SPH exhibits a stabilizing effect on SM/CHOL domains.

These results show convincingly how CER and SPH dramatically change the domains morphology and their organization in the membrane plain. As demonstrated by our results, CER and SPH show lower miscibility with other lipids. CHOL readily melts CER and SPH in a GPL environment. The presence of SM in quaternary mixtures (PC/SM/CER/CHOL) stabilizes the gel phase and thus decreases CER miscibility. More concurrent CER/SM interactions induce a change in the conditions of  $L_o$  phase formation (SM/CHOL interactions). SPH shares similar behavior with CER but at a much lower degree. Direct incorporation of CER and SPH in ternary raft mixtures (at least 20 mol% CHOL and SM) induced significant

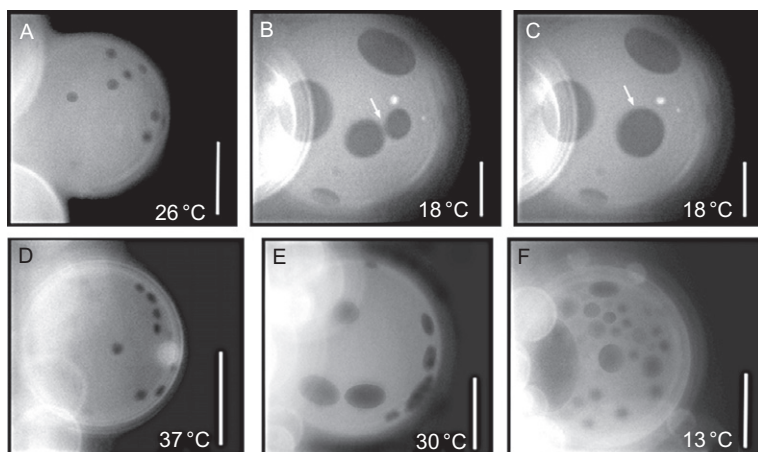


**Figure 7.6**  $L_o/L_d$  phase separation in a PC/SPH/SM/CHOL 40/20/20/20 quaternary mixture (A–C). Formation of  $L_o$  domains at about 26 °C (A). Domains before (B) and after fusion (C).  $L_o/L_d$  phase separation in PC/SPH/SM/CHOL 30/20/30/20 (D–F). Formation of  $L_o$  domains at physiological temperature (D). Increasing domain number and size with decreasing temperature (E and F). The headgroup-labeled lipid analogue  $L$ - $\alpha$ -phosphatidylethanolamine-*N*-(lissamine rhodamine B sulfonyl) was used to visualize the phase coexistence Bar 20  $\mu\text{m}$ . Reprinted from Ref. [82] with permission from Elsevier.

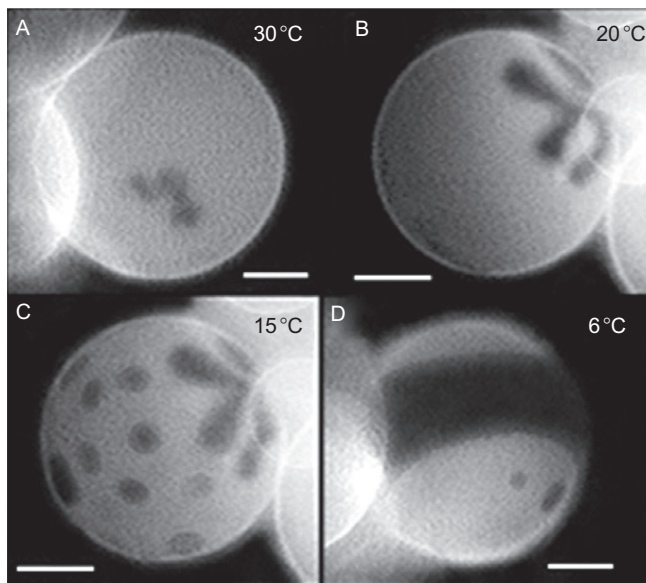


**Figure 7.7** Domain pattern as a function of temperature of the quaternary PC/SM/CER/CHOL 50/17.5/15/17.5 mixture. Dark irregular domains formed at about 36 °C. For better visibility, domains are present at 30 °C (A). Well-formed leaf-like domains were observed at 20 °C (B). Round-shaped domain in  $L_o$  phase appeared at 17 °C and band-like domains at low temperatures (D). The observation of dark leaf-like and round-shaped domains is consistent with  $L_\beta/L_o/L_d$  phase coexistence at 15 °C for this composition (C). The fluorescent lipid analogue acyl 12:0 NBD PC (1-acyl-2-{12-[(7-nitro-2-1,3-benzoxadiazol-4-yl) amino]dodecanoyl}-sn-glycero-3-phosphocholine) was used to visualize the phase coexistence. Bar 20  $\mu\text{m}$ . Reprinted from Ref. [80] with permission from Elsevier.

enlargement of the  $L_o$  phase. Surprisingly, the dark spots preserve their liquid-like properties even at a high CER and SPH content.

All these results support the hypothesis that CER and SPH can promote the formation of large signaling platforms if this concerns the micron scale.



## 4. VISUALIZATION OF ENZYME ACTIVITY IN BIOMIMETIC SYSTEMS

### 4.1. Sphingomyelinases

#### 4.1.1 Brief description of SMases

SMases are enzymes that catalyze the hydrolysis of SM into CER and phosphorylcholine (Fig. 7.2). The reaction is formally similar to that of phospholipase C. SMases have been known for many years but in the past decade they have become the object of renewed interest after the discovery

of the SM signal transduction pathway [89]. CER can be generated within a cell either through a *de novo* synthesis pathway mediated by CER synthase or through hydrolysis of cellular SM via an acid or neutral SMase. There is evidence to suggest that both these pathways are involved in CER generation in response to different stimuli. Different SMases have been described in mammalian cells, tissues, and biological fluids [72]. Up till now, seven SMases have been distinguished: (1) acid SMase (lysosomal SMase); (2) neutral, membrane-bound Mg-dependant SMase (nervous tissues); (3) neutral, Mg-independent SMase (myelin sheath); (4) neutral, Mg-, and dithiothreitol-stimulated SMase (human cells); (5) neutral SMase (chromatin); (6) alkaline SMase (bile and digestive tract); and (7) Zn-dependent SMase (serum).

Three stages could be distinguished in the enzyme activity to describe the interaction of SMases with its substrate [90]: (1) a latency period during which interfacial adsorption and other precatalytic steps took place, (2) a period of steady-state enzyme activity, and (3) a period of gradual halting of product formation.

The role of SMases exceeds the originally proposed one in the intermediary metabolism of lipids. Nowadays, SMases are related to cell processes such as apoptosis, cell proliferation, cell differentiation, and membrane fusion/fission. Current biophysical studies based on biomimetic systems are focused on the plausible explanations for the physiological effects of these enzymes. Aspects that attract scientific attention are how a heterogeneous membrane structure, with lateral domains in the membrane, is able to modulate enzyme activity, enzyme-mediated vesicle transformations, membrane permeability and, vice versa, how enzyme activity could reorganize the coexisting phases.

#### **4.1.2 SMase activity in homogeneous and heterogeneous GUV membranes**

Historically, the study of Holopainen *et al.* [45] represents the first demonstration of vectorial formation of vesicles, that is, endocytosis-like and shedding, to be induced by the asymmetrical formation of CER by exogenous SMase in either the outer or inner leaflet, respectively, of PC/SM giant vesicles. The asymmetric accumulation of CER closely resembles the mechanism of CER generation which takes place *in vivo* before triggering other cellular responses. Later, Taniguchi *et al.* [91] showed the SMase activity on heterogeneous DOPC (1,2-dioleoyl-*sn*-glycero-3-phosphocholine)/C<sub>16</sub>-CER/C<sub>16</sub>-SM/CHOL vesicles. The L<sub>o</sub>/L<sub>d</sub> phase coexistence was

transformed into an  $L_{\beta}/L_d$  one. Our own results demonstrated how an  $L_o/L_d$  membrane, with microdomains in the membrane plane, is reorganized and dynamically controlled by SMase enzyme activity in six macroscopically resolved stages [80]. To study the consequences of the enzymic conversion of SM into CER in a heterogeneous membrane, we treated GUV, prepared from PC/SM/CHOL 60/22.5/17.5 mixtures, with SMase (Fig. 7.8). The injection of the enzyme adjacent to the external membrane surface enabled the space around the vesicle to be saturated with SMase. The SM to CER conversion resulted in the following macroscopically resolved stages during the

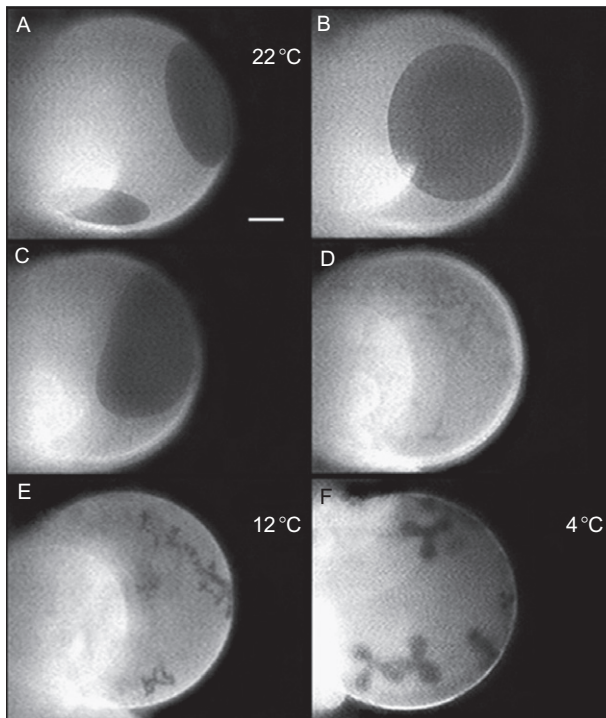


**Figure 7.8** Hydrolysis of sphingomyelin by sphingomyelinase in heterogeneous  $L_o/L_d$  membrane of GUVs composed of PC/SM/CHOL (60/22.5/17.5) at 22 °C. Visualization of  $L_o/L_d$  phase coexistence (A).  $L_o$  domain fusion after enzyme microinjection (B). After 5–10 min, appearance of significant  $L_o$  border undulations, transformation of round-shaped  $L_o$  domains into elongated ones (C).  $L_o$  domain disintegration and formation of irregular channel-like domains between 10 and 20 min after the enzyme injection (D). Leaf-like domain formation with two, three, or four petals was observed at lower temperatures (E and F). The same vesicle is presented in the series of images. The fluorescent lipid analogue acyl 12:0 NBD PC (1-acyl-2-{12-[(7-nitro-2-1,3-benzoxadiazol-4-yl) amino]dodecanoyl}-sn-glycero-3-phosphocholine) was used to visualize the phase coexistence. Bar 20  $\mu\text{m}$ . Reprinted from Ref. [80] with permission from Elsevier.

course of enzymic activity: (1) fusion of  $L_o$  domains where more than one domain exists (Fig. 7.8A and B); (2) appearance of noticeable  $L_o$  border undulations (Fig. 7.8B and C); (3) loss of circular shape of the  $L_o$  domains and appearance of elongated ones (Fig. 7.8C); (4) disintegration of  $L_o$  domains, subsequent reorganization of membrane phases, and transformation of  $L_o/L_d$  phase separation into  $L_\beta/L_d$ . Formation of irregular gel-like domains in the form of a narrow channel on the bright background (Fig. 7.8D and E); (5) reorganization of the dark fraction and formation of leaf-like gel domains with two or three petals at low temperatures (4 °C) (Fig. 7.8F); and (6) membrane invagination or vesicle collapse upon addition of more enzyme (data not shown). In cases when the SM content was large enough (PC/SM/CHOL 45/45/10), SMase activity on a  $L_o/L_d$  membrane at 37 °C induced initially a bright  $L_d$  invagination and accumulation of small daughter vesicles in the mother vesicle, which did not allow further clear detection of  $L_o$  domains by the epifluorescence method. This result was not unexpected because Holopainen *et al.* [45] have reported similar invaginations in PC/SM GUV membranes. Apparently, in PC/SM/CHOL 45/45/10 mixture, the  $L_d$  phase (bright region) was highly enriched in SM and this bright region, already enriched in CER due to SMase action, was more susceptible to inward curvatures compared to the stiff  $L_o$  phase.

Fluorescence microscopy of free-standing GUV allowed visualization of the SMase activity on  $L_o/L_d$  heterogeneous membrane. Round-shaped  $L_o$  domains were transformed into narrow channel-like ( $L_\beta$ ) domains on the bright background during the first 20–30 min of SM conversion into CER and these domains were stable at least for 1 h after their formation. It should be mentioned that in this case the lipid system is out of thermodynamic equilibrium because of continuous enzyme activity and asymmetric generation of CER in comparison with the predefined quaternary mixtures (PC/SM/CER/CHOL). The processes of membrane reorganization are controlled by the lateral and transverse diffusion of the lipids at the time scale of our experiment. It is known that CER has a comparatively rapid flip-flop movement compared with other lipids (half-time of 22 min at 37 °C for fluorescent analogue of CER [92] and half-time of approximately 1 min at the same temperature for unlabeled-C16 CER [93]). Despite the rapid flip-flop of CER, it is difficult to make some comparisons between dynamically controlled lipid systems, which are out of equilibrium because of continuous asymmetric CER generation and predefined mixtures in thermodynamic equilibrium. However, the gel phase morphology induced after SMase action, that is, formation of domains with three petals, appears like a phase

separation in 50/30/10/10 PC/SM/CER/CHOL mixture, indicating that the SM/CER ratio could be approximately 3/1.

Lopez-Montero *et al.* [94] went even further in analyzing the effect of SMase action on the membrane lateral tension. Formation of membrane defects and total vesicle collapse at relatively low percentage of SM ( $\approx 5$  mol%) has been observed. Vesicle rupture was prevented when GUVs were composed of raft-like mixtures (PC/PE/SM/CHOL) and in the presence of lysophosphatidylcholine (LysoPC) (5 mol%). With enzyme activity, raft-containing PC/PE/SM/CHOL vesicles exhibiting peanut shape became spherical. The overall morphological changes suggest that SMase induces a lateral tension caused both by the asymmetrical SM distribution following SMase treatment and by the condensing effect of the newly formed CER.

A link between the bulk (cuvette) studies of lipase activity on lipid bilayers in different physical states and the morphological data obtained with GUV was recently made by Ibarguren *et al.* [95]. The authors found that SMase binding to the vesicles appears to be a slow and random process (several minutes) but the catalytic activity follows rapidly. They suggest a “scooting” mechanism for the hydrolytic activity and generalize that the enzyme preferentially binds fluid-disordered domains over fluid-ordered or gel domains. At this point, it is better to distinguish the two kinds of experiments that can be carried out in GUV enzyme experiments: adding the enzyme to the GUV chamber (similar to the bulk studies) and local microinjection of the enzyme at proximity of the GUV membrane. The second procedure allows direct enzyme delivery onto/or close to the micron-scale raft-like domains. This difference in the enzyme delivery might be a reason why Taniguchi *et al.* [91] and we [80] observed the disintegration of  $L_o$  domains after the enzyme delivery and only transformation of peanut-shaped  $L_o/L_d$  vesicles to spherical ones in the experiments of Lopez-Montero *et al.* [94] and Ibarguren *et al.* [95].

A recent study showed in particular an elegant way for sphingomyelinase D (*loxosceles* spider venom) activity in homogeneous and heterogeneous GUV experiments in symbiosis with LUV experiments [96]. This enzyme transforms SM to ceramide-1-phosphate. The effects of ceramide-1-phosphate on model membranes were studied both by *in situ* generation of this lipid using a SMase D and by premixing it with SM/CHOL mixtures. The authors demonstrated that ceramide-1-phosphate is able to generate coexistence of liquid-disordered/solid-ordered phases in SM/ceramide-1-phosphate mixtures. The micron-sized  $L_o$  domains formed in GUV composed of DOPC/eggSM/CHOL mixture disappeared after enzymatic generation of

ceramide-1-phosphate. It is suggested that CHOL presence counteracts the structural effects of the enzymic product. Accordingly, this study showed that the impact of ceramide-1-phosphate on membrane organization depends on its composition and SMase D may have different effects on different cellular targets.

In summary, all these results represent a clear real-time visualization of the correlation between SMase activity and the changes in membrane organization as well as vesicle topologies. The generation of CER from raft-containing SM induces disintegration of these assemblies and formation of CER-enriched gel domains. The generation of CER in  $L_d$  phase induces inward/outward budded small vesicles and/or shrinking/collapse of the targeted vesicles. Enzyme activity by alteration of local/nonlocal lipid composition is able to modulate long-range lipid organization in the membrane plane. These experiments are in accordance with the newly identified function of CER to be a principal modulator of the membrane structure participating in the domain coalescence, receptor clustering, and vesicle formation.

## 4.2. Phospholipases A2

### 4.2.1 Brief description of phospholipases A2

Phospholipases A2 (PLA2) are a family of ubiquitous, small, and water-soluble lipolytic enzymes. PLA2 catalyzes the hydrolysis of the *sn*-2 ester bond of membrane phospholipids to liberate fatty acid and lysophospholipid (Fig. 7.9). One of these products, arachidonic acid, is transformed into potent

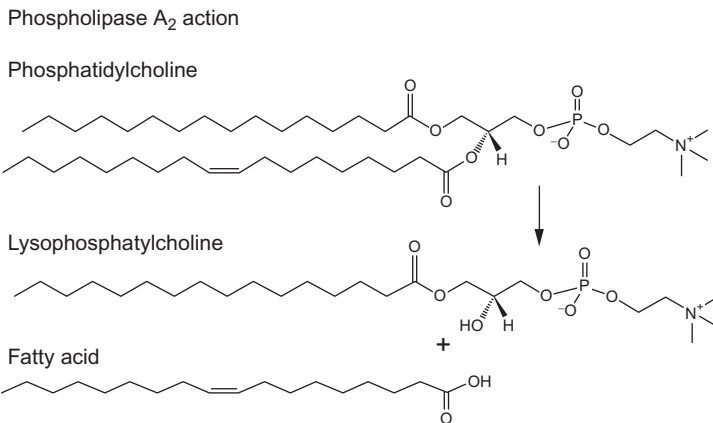


**Figure 7.9** Phospholipases A2 catalyzes the hydrolysis of the *sn*-2 ester bond of the glycerophospholipids to liberate fatty acid and lysophospholipid. Lipid structures were taken from the LIPID MAPS Lipidomics Gateway [65].



inflammatory lipid mediators, collectively known as eicosanoids. Multiple forms of PLA2, including secretory PLA2 (sPLA2) and  $\text{Ca}^{2+}$ -dependent cytosolic PLA2, and  $\text{Ca}^{2+}$ -independent intracellular PLA2, have been identified in mammalian tissues. Secretory type II PLA2 and intracellular PLA2s, group IVA cytosolic phospholipase A2, have been shown to be involved in inflammation, whereas intracellular PLA2 has been implicated in spermatogenesis and insulin signaling.

The enzyme activity is often measured via its peculiar lag-burst kinetics. PLA2 hydrolysis is characterized by a latency period, that is, a period of low activity, followed by a burst in activity. The burst has been suggested to be caused by the accumulation of hydrolysis products, free fatty acid, and LysoPC, created during the latency period. In turn, the enzyme products alter the susceptibility of the phospholipid membranes to PLA2-induced degradation.

Results obtained from a variety of experimental and theoretical studies of secretory PLA2 activity on lipid bilayer substrates have provided insight into the dependence of the enzyme activity on bilayer composition, lateral structure, and thermodynamic conditions [97].

The hypothesis of raft existence in cell membranes raises immediately questions about the activity of PLA2 on the raft and non-raft regions of the membrane, as well as in the vicinity of the interphase boundary, due to their different molecular composition and packing. Yet, the possible relationship between enzymatic changes in lipid composition and changes in phase morphology and vesicle shape transformations has not been well investigated.

#### **4.2.2 Phospholipase A2 activity in homogeneous and heterogeneous GUV membranes**

The pioneering work devoted to the PLA2-mediated vesicle transformations belongs to Wick *et al.* [43]. Addition of the enzyme (PLA2 from venom of the cobra snake *Naja naja*) to the outside of a homogeneous substrate vesicle (1-palmitoyl-2-oleoyl-*sn*-glycero-3-phosphocholine) caused it to burst, whereas injection of the enzyme inside a vesicle resulted in a slow and constant decrease in its size, until it eventually disappeared from the resolution limit of the light microscope.

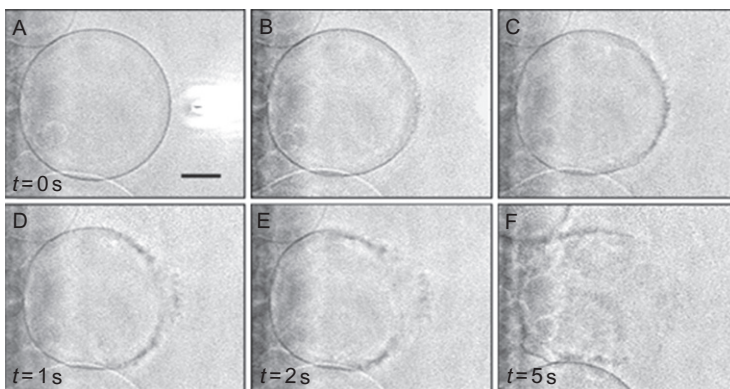
Later, a two-photon view of PLA2 (*Crotalus atrox* venom) acting in single-lipid and in gel/liquid-disordered GUV was provided by Sanchez *et al.* [46]. Independent of the lipid composition, all GUVs reduced their size as sPLA2-dependent lipid hydrolysis proceeded. A preferential binding of the enzyme to the liquid regions was found at temperatures promoting domain

coexistence. sPLA2 hydrolyzes the liquid domains in the binary lipid mixtures 1,2-dilauroyl-*sn*-glycero-3-phosphocholine/DAPC (1,2-diarachidoyl-*sn*-glycero-3-phosphocholine) and 1,2-dimyristoyl-*sn*-glycero-3-phosphocholine/DMPE (1,2-dimyristoyl-*sn*-glycero-3-phosphoethanolamine), indicating that the solid-phase packing of DAPC and DMPE interferes with sPLA2 binding, irrespective of the phospholipid headgroup. These studies emphasize the importance of lateral packing of the lipids in sPLA2 enzymatic hydrolysis of the membrane.

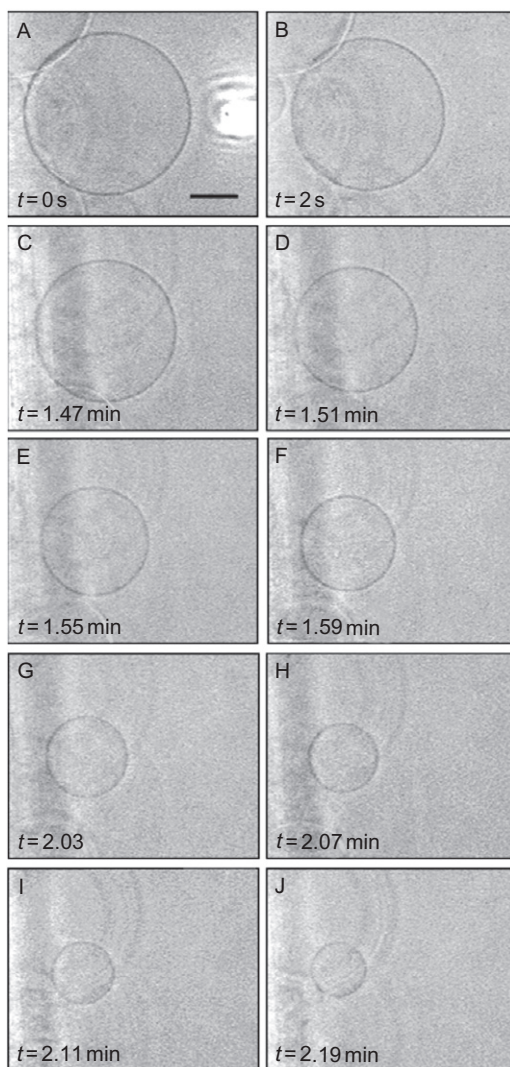
The activity of sPLA2 (from *bee* venom) in raft-containing GUV, with and without CER, was studied by Staneva *et al.* [47,80,98]. Systematic investigations of PLA2 action on GUV composed of single-substrate lipid (PC), binary (PC/SM), ternary (PC/SM/CER and PC/SM/CHOL), and quaternary mixtures (PC/SM/CER/CHOL) were carried out. Total fragmentation of PC vesicles was observed by formation of smaller ones only 5 s after the enzyme microinjection in the vesicle proximity (Fig. 7.10) [98].

A wide variety of discontinuous vesicle shapes and topology transformations were observed upon varying the amount of enzyme (Fig. 7.11, half of the enzyme amount was added compared to Fig. 7.10).

In contrast, sPLA2 treatment of PC/SM 50/50 GUVs did not induce significant transformations in vesicle shape where no apparent macroscopic phase separation was detected at 37 °C (Fig. 7.12). Only slight vesicle shrinking, resulting from partial hydrolysis, was observed. This process, however, was rapidly ended and the vesicles regained their initial size. Apparently, the presence of SM in the model membranes augmented membrane resistance to sPLA2. This could be attributed to the inhibitory effect of SM on this enzyme.

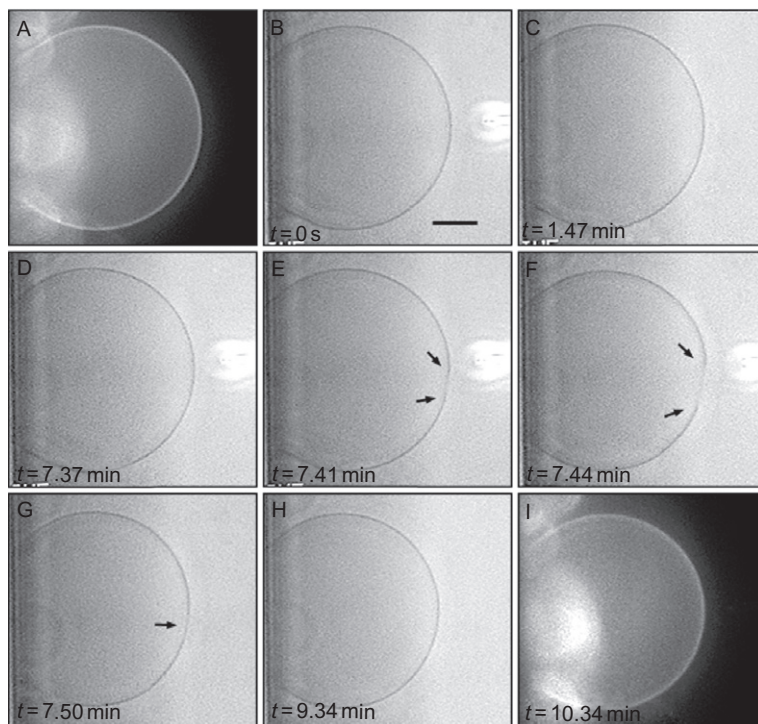


**Figure 7.10** sPLA<sub>2</sub> activity on GUVs composed of egg PC which serves as enzyme substrate at 20 °C. Burst of the vesicle is observed. Bar 20 μm. Reprinted from Ref. [98].



**Figure 7.11** sPLA<sub>2</sub> activity on GUVs composed of egg PC at 20 °C. Shrinking of the vesicle is observed. Bar 20 μm. Reprinted from Ref. [80] with permission from Elsevier.

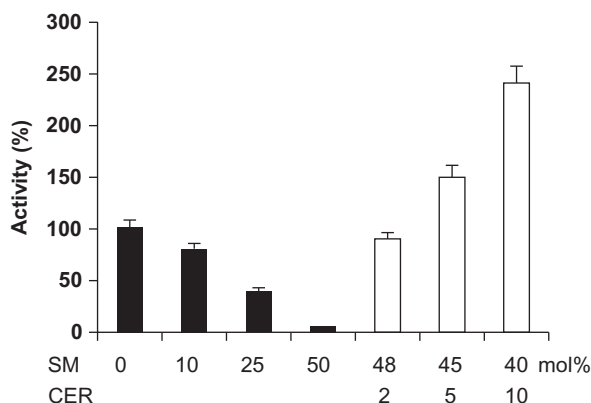
To assess enzyme activity, similar investigations were performed with SUV having the same phospholipid composition (Fig. 7.13). These liposomes were incubated in the presence of *bee* venom sPLA<sub>2</sub>, the enzyme activity being measured by determination of the liberated fatty acids. The activity of sPLA<sub>2</sub> hydrolyzing SUV-containing egg PC was considered as 100%. By elevation of the SM level incorporated into these liposomes,



**Figure 7.12** sPLA<sub>2</sub> activity on GUVs composed of PC/SM 50/50 at 37 °C. The vesicles retain their initial shape. The lipid analogue acyl 12:0 NBD PC (1-acyl-2-[[7-nitro-2-1,3-benzoxadiazol-4-yl]amino]dodecanoyl]-*sn*-glycero-3-phosphocholine) was used for fluorescence. Bar 20  $\mu$ m. Reprinted from Ref. [98].

the activity gradually decreased. At a ratio PC/SM 50/50, the enzyme activity was inhibited almost completely (96% inhibition).

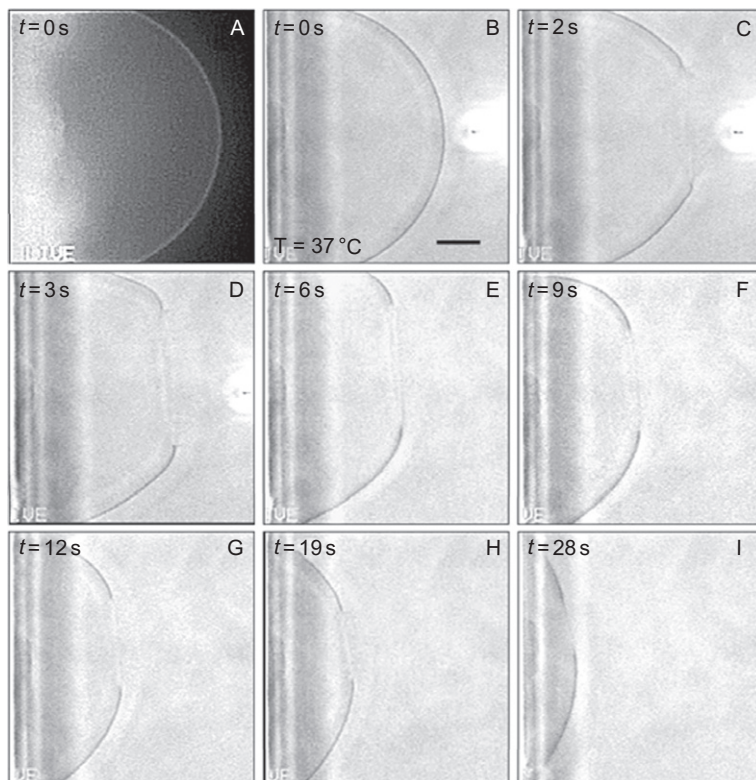
When a small fraction of SM (2%) was replaced with CER, an appearance of a hole in the membrane bilayer and a sharp reduction in vesicle diameter was observed (Fig. 7.14). This suggests a more rapid rate of substrate hydrolysis in the presence of CER. Obviously in this case, the reaction did not proceed at the same rate as in GUVs of egg PC (about 5 s), but still an almost complete vesicle disintegration was observed in about 28 s. Vesicle rupture was observed when 5 mol% SM was replaced by 5 mol% CER (data not shown). The replacement of SM by 2, 5, and 10 mol% CER induced enzyme reactivation of sPLA<sub>2</sub> (Fig. 7.13). The exact mechanism of the observed sPLA<sub>2</sub> activation by CER is still unknown. The consensus opinion is that this activation is due to formation of gel nanodomains when the concentration of CER is at least 5% [99]. Our studies (Fig. 7.13) showed that this



**Figure 7.13** sPLA<sub>2</sub> activity on SUVs composed of egg PC and different concentrations of SM and CER. Determination of released fatty acids (C<sub>20:4</sub>) was performed by GC-MS. Values represent means  $\pm$  SD of three determinations of two independent experiments. Reprinted from Ref. [98].

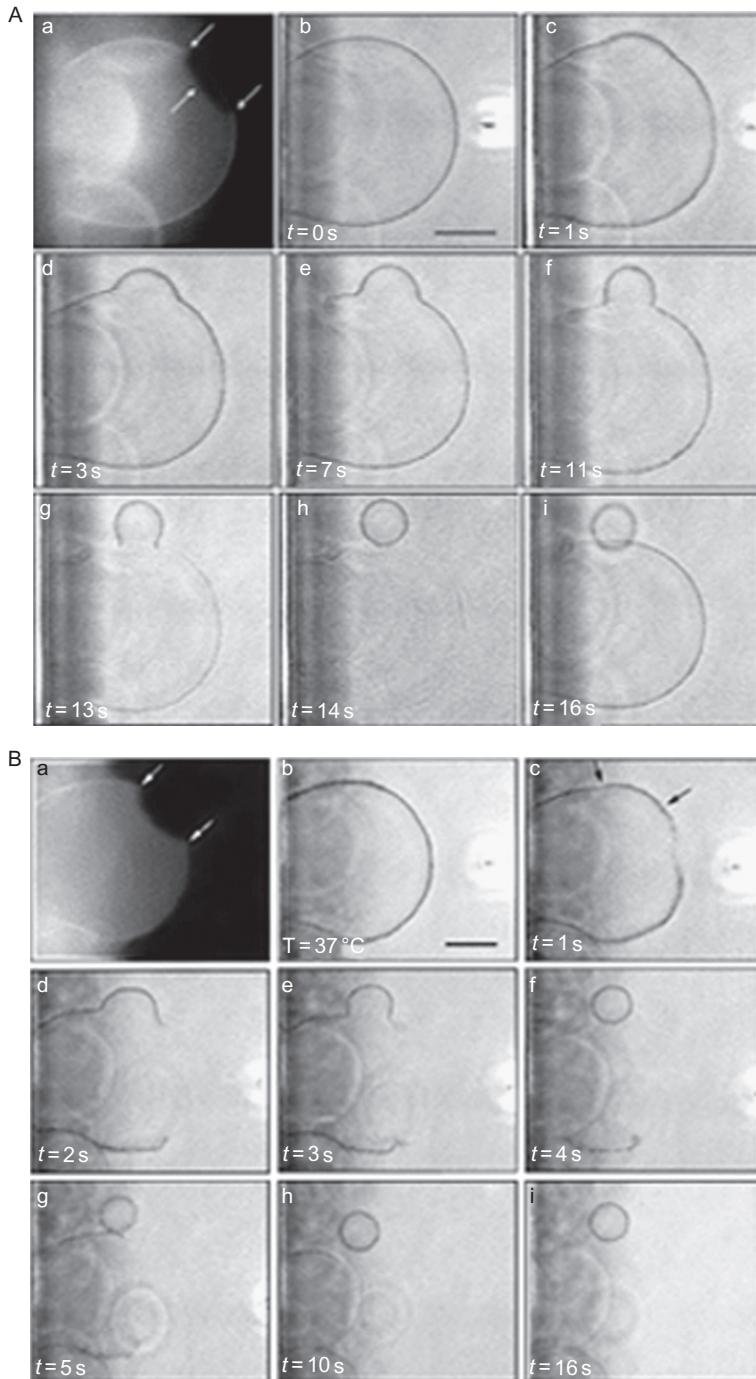
activation occurs even at 2% CER. It was presumed that CER up to 2% is not sufficient to form domains, but CER molecules serve as nucleation sites for enzyme insertion into the substrate bilayer. However, in SM-enriched mixtures, SM tends to stabilize these domains by formation of stable complexes with CER [81]. Thus, CER sequesters SM, a sPLA<sub>2</sub> inhibitor, making the phospholipid substrate more susceptible to enzyme attack.

In control “raft” PC/SM/CHOL 45/45/10 mixture, sPLA<sub>2</sub> activity induced continuous L<sub>o</sub> domain budding and fission without appearance of holes or L<sub>d</sub> membrane fragmentation (Fig. 7.15A) [47]. When the CHOL content was augmented in ternary mixtures, increasing amounts of SM were engaged in the dominant SM/CHOL interactions, resulting in an increase of L<sub>o</sub> domain formation (data not shown). In contrast, the L<sub>d</sub> phase became more SM depleted. Thus, the presence of CHOL seemed to relieve the inhibitory effect of the latter [100] and the L<sub>d</sub> phase became more susceptible to PLA<sub>2</sub> hydrolysis (Fig. 7.16). The budding process in PC/SM/CER/CHOL (45/43/2/10) mixture was triggered within 1 s after sPLA<sub>2</sub> injection (Fig. 7.15B, c) whereupon it developed (Fig. 7.15B, d and e) and was finalized after about 4 s by fission of raft-like L<sub>d</sub> domains (Fig. 7.15B, f). The L<sub>d</sub> phase was completely disintegrated after 16 s (Fig. 7.15B, f–i) in contrast to the L<sub>o</sub> phase, which remained intact. As described already, the presence of relatively low proportions of CER induces significant morphological vesicle transformations after sPLA<sub>2</sub> treatment, unlike in PC/SM vesicles.



**Figure 7.14** sPLA<sub>2</sub> activity on GUVs composed of PC/CER/SM (50/2/48) at 37 °C. Pore opening and vesicle membrane fragmentation are observed. The lipid analogue acyl 12:0 NBD PC (1-acyl-2-[12-((7-nitro-2-1,3-benzoxadiazol-4-yl)amino)dodecanoyl]-sn-glycero-3-phosphocholine) was used for fluorescence. Bar 20  $\mu\text{m}$ . Reprinted from Ref. [98].

It should be noted that the vesicle response is not only due to the enzyme activity but also due to the material properties of vesicle membranes. Nevertheless, we established a correlation between the enzyme activity and the vesicle morphological transformations [98]. It can be seen from Figs. 7.13 and 7.16 that increasing the SM concentrations in substrate vesicles leads to progressive decrease in PLA<sub>2</sub> activity, while CER presence increases the enzyme activity. CHOL relieves the inhibitory effect of SM (Fig. 7.16) [100,101]. Thus, one can imagine that at least two patches are formed in the heterogeneous membrane: substrate and nonsubstrate sites unlike a homogeneous PC/SM membrane. Cohesive forces in homogeneous membranes, even after substrate hydrolysis, are apparently stronger compared to heterogeneous membranes (PC/SM/CER or PC/SM/CER/CHOL),



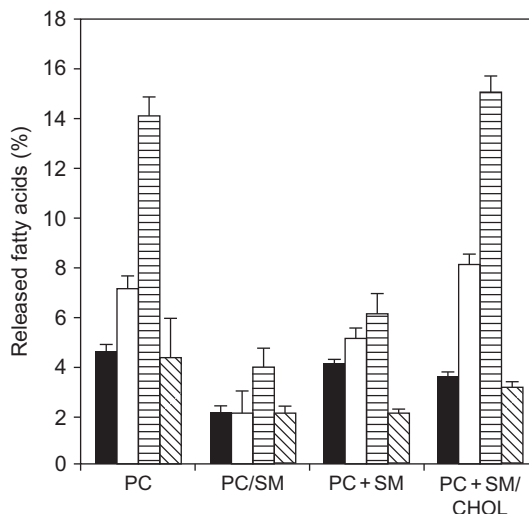


**Figure 7.16** cPLA<sub>2</sub> activity on PC, PC/SM (70/30) vesicles, or cPLA<sub>2</sub> was pre-incubated with SM (PC + SM) or SM/CHOL (PC + SM/CHOL) vesicles and then added to incubation medium containing PC vesicles. Determination of released fatty acids (C<sub>18:1</sub>, filled columns; C<sub>20:4</sub>, open columns; C<sub>22:6</sub>, striped columns; C<sub>22:6</sub>, hatched columns) was performed by GC-MS. Values represent means  $\pm$  SD of three determinations of two independent experiments. Reprinted from Ref. [101] with permission from the American Society for Biochemistry and Molecular Biology.

where substrate patches are converted into products (LysoPC and fatty acid). The tensile strength (cohesive forces) of the membrane decreases with increasing LysoPC concentration [102]. This decrease in the membrane strength determines the substantial decrease in the necessary work for membrane breakdown. For example, an increase in the LysoPC concentration above 50 mol% results in an apparent disappearance of the spontaneously formed bilayer structures and their replacement by micellar structures.

**Figure 7.15** sPLA<sub>2</sub> activity in control "raft" PC/SM/CHOL (45/45/10) mixture induces continuous L<sub>o</sub> domain budding and fission (A) [47]. sPLA<sub>2</sub> activity in CER-containing raft mixture (PC/SM/CER/CHOL (45/43/2/10)) (B) [80]. One second after sPLA<sub>2</sub> injection, the budding process triggers (B, c), develops (B, d and e) and after about 4 s finalizes by fission of raft-like liquid-ordered domain (B, f). L<sub>o</sub> phase is completely disintegrated for 16 s (B, f-i) in contrast to the L<sub>o</sub> phase which remains intact. The same vesicle is presented in the series of images. The fluorescent lipid analogue acyl 12:0 NBD PC (1-acyl-2-{12-[(7-nitro-2-1,3-benzoxadiazol-4-yl)amino]dodecanoyl}-sn-glycero-3-phosphocholine) was used to visualize the phase coexistence. Bar 20  $\mu$ m. Reprinted from Ref. [47,80] with permission from Elsevier.



Overall, these results demonstrate how CER and CHOL sequester SM, a sPLA2 inhibitor, making the phospholipid substrate more susceptible to enzyme attack. CER and CHOL are able to modulate sPLA2 activity and the processes such as membrane fragmentation, budding in, and budding out by inducing changes in the lipid organization of the bilayer.

#### **4.2.3 A possible mechanism for raft vesicle budding and fission**

To propose a plausible mechanism for raft-like vesicle budding and fission, the following experiments were carried out to confirm or reject the hypothesis that the enzyme-generated LysoPC seems to be the key molecule for the fission mechanism.

##### **4.2.3.1 Threshold sPLA2 activity is needed to trigger the $L_o$ domain fission**

Raft vesicle fission, but not raft budding, is critically dependent on the PLA2 enzymatic activity [47]. So, addition of inactive or poorly active enzyme still initiates raft budding from the initial raft-GUV but the process does not develop to the completion of the final fission and raft vesicle expulsion. As sPLA2 is a  $Ca^{2+}$ -dependent enzyme, the addition of EDTA to the enzyme solution is a common way to inhibit enzyme activity. Lowering the temperature leads to decrease of the enzyme activity as well. In both cases, initial budding at the raft sites appears temporally after local PLA2 addition, but then reverses upon enzyme diffusion. The raft domains remain in the original vesicle.

Our experiments indicate that the presence of  $L_o$  domains (rafts) *per se* is not sufficient for budding to appear even from a tension-free (fluctuating) GUV. In contrast, the adsorption of sPLA2 could trigger budding at the raft sites. The destabilizing effect of sPLA2 might be due to modification of the local spontaneous curvature of the membrane in both ( $L_o$  and  $L_d$ ) phases. Externally added sPLA2 adsorbs onto the vesicle membrane in an asymmetrical way since the enzyme cannot cross the bilayer. Due to the asymmetrical constraint generated on the coupled lipid bilayer, the partial penetration of PLA2 molecules into the external leaflet is likely to induce a spontaneous curvature (i.e., a budding toward the exterior). Difference in the protein adsorption between  $L_o$  and  $L_d$  phases, as well as surface tension modifications at the lipid bilayer/water interface, might also contribute to the effect. However, this is the place to mention that a complete sPLA2 inhibition cannot be achieved and it is not possible to observe properly the effect of inactive PLA2 on  $L_o/L_d$  membranes. Thus, we can conclude that fission of the budded vesicle could only be observed at threshold enzyme activity and therefore

requires the presence of one or both of its reaction products. This prompted us to examine the effect of LysoPC alone on the  $L_o$  domain budding and fission. The LysoPC, because of its special molecular shape of an inverted cone, merits more special attention compared to the fatty acid.

#### 4.2.3.2 LysoPC characterized with its inverted cone molecular shape is the key to the fission mechanism

LysoPC solution at different concentrations was injected in the proximity of the vesicle surface [103] (Fig. 7.17). At exogenous low LysoPC concentrations, we observed a rise of thermal fluctuations of both raft and non-raft regions of the membrane, which was not the case when sPLA2 was injected.

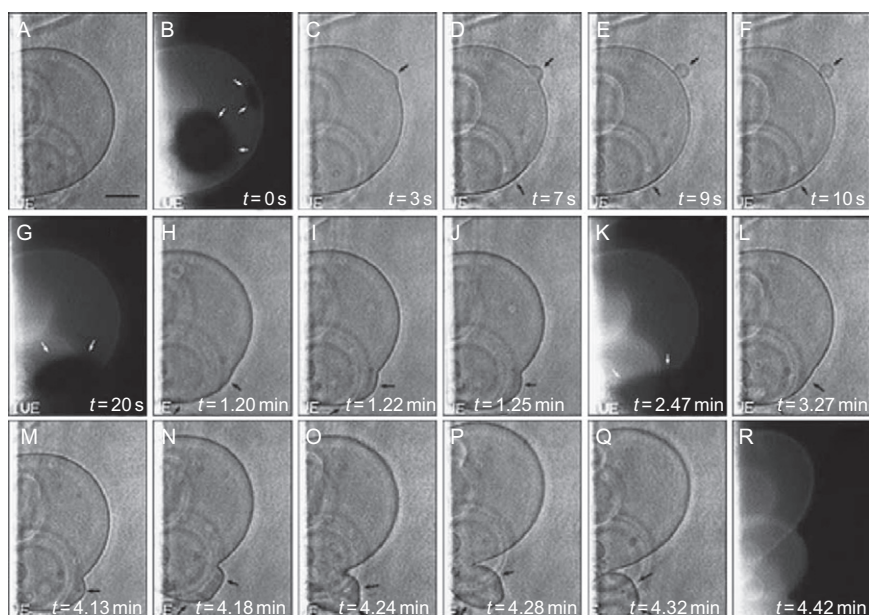


**Figure 7.17** Raft-like domain budding and fission promoted by LysoPC from *GUV* composed of PC/SM/CHOL (45/45/10) at 30 °C. The first injection of LysoPC was sufficient to trigger the process of  $L_o$  domain budding and fission for the small domain (A–G): (A) initial raft–*GUV* in phase contrast, (B) the white arrows point at two dark  $L_o$  domains: a small one (about 10  $\mu\text{m}$  in diameter) and a big one (30  $\mu\text{m}$ ); (C–F) microinjection, small  $L_o$  domain budding and complete fission; (G) no small dark domain left in the mother vesicle (the fission was completed in 10 s). The large domain fission was achieved neither after the first (A–G) nor after the second (H–L) LysoPC injection. It was the third one which succeeded in getting the fission completed (M–R). Bar: 20  $\mu\text{m}$ . The fluorescent lipid analogue acyl 12:0 NBD PC (1-acyl-2-[12-[(7-nitro-2-1,3-benzoxadiazol-4-yl) amino]dodecanoyl]-sn-glycero-3-phosphocholine) was used to visualize the phase coexistence. Reprinted from Ref. [103] with permission from Elsevier.

That suggests partition of the exogenous LysoPC concentrations into both  $L_d$  and  $L_o$  phases. LysoPC is able to trigger the budding of the small  $L_o$  domain and leads to its complete fission as an  $L_o$  phase vesicle, as shown in Fig. 7.17C–F. A further indication that budding involves the  $L_o$  domain is the simultaneous disappearance of the small dark spot in the parent vesicle (Fig. 7.17G). As seen from Fig. 7.17G, the larger  $L_o$  domain remains in the parent vesicle. Fission of this latter domain was not achieved even by a second LysoPC injection (Fig. 7.17H–L), although a limited and reversible budding was apparent. It was only the third LysoPC injection that succeeded in yielding a complete fission of the domain (Fig. 7.17M–R). Increased membrane thermal fluctuations of the  $L_d$  and  $L_o$  membranes were occasionally observed during the larger  $L_o$  domain budding (Fig. 7.17M–P). This is presumably due to bilayer bending rigidity decrease after LysoPC incorporation and/or to internal pressure decrease of the more tense vesicles that results from water efflux due to transient membrane opening.

The data described above illustrate a general trend in our experiments, namely that small domains required less LysoPC molecules to undergo complete budding than large domains.

Therefore, any other cone-shaped molecules such as detergents could induce the same or similar effects as the natural detergent in cell, LysoPC.

#### 4.2.3.3 Other cone-shaped molecules such as detergents should also induce $L_o$ domain budding and fission

Indeed, the detergents, Triton X-100 and Brij 98, were also able to induce both budding and fission of  $L_o$  domains from GUV as the active sPLA2 did [103]. The solubilization of the  $L_d$  phase occurs more slowly and is not correlated in time with the budding since the solubilization occurs while budding is already in progress.

Triton X-100 is known as the most typical and strongest detergent for low temperature raft extraction which yields detergent-resistant membranes (DRMs) highly enriched in SM and CHOL. Brij 98 is a milder and moderately selective detergent, which yields less selectively enriched DRMs at 37 °C, which appear to be similar in composition [104] to the so-called non-detergent lipid rafts [105].

To the extent that  $L_o$  domains can be considered as models for rafts in biomembranes, our work has several biological consequences. First, we observed neither domain formation nor domain coalescence to be induced by the addition of detergents to GUVs. Our experiments suggest that the  $L_d$  phase is more susceptible to solubilization as is observed for the preparation

of DRMs. Therefore, the experiments presented here support the idea that (i) no detergent-associated artifacts occur during isolation of DRM from cells and (ii) temperature effects may occur (it cannot be ruled out that the low temperature used in Triton X-100 extraction may have an effect on raft size). It is in fact possible that DRM exclusion from cells occurs as it is observed here, that is, by budding of rafts prior to solubilization of the non-raft membranes.

#### 4.2.3.4 Possible mechanism for domain budding and fission

We propose a possible mechanism for PLA2 and detergent-induced vesiculation of rafts that relates first, to several distinct physicochemical properties of a multicomponent lipid membrane which contains domains, and second, to the inverted cone-shaped molecules (LysoPC, Triton X-100, and Brij 98). Indeed, budding appears to be an intrinsic property of multicomponent membranes [106]. In a two-phase membrane, the difference in composition of the two phases is usually associated with a difference in spontaneous curvature, as well as with a free energy term, which is proportional to the length of the interphase boundary (the density of this free energy term being the line tension at interphase boundary). In general, both the spontaneous curvature and the line tension provide a driving force for budding of one domain from the lipid bilayer matrix and it leads to a decrease of the length of the interphase boundary. Whether budding actually occurs is related to the interplay with the opposing effect of bending free energy, in the general case, on any mechanical lateral tension applied on the membrane [106]. Budding occurs preferentially at the  $L_o$  domains since it also has the effect of decreasing the boundary between the two phases, a process that is also energetically favorable (e.g., due to differences in  $L_o/L_d$  bilayer thickness) [107].

The direction of the bending (the budding direction) is determined by the asymmetrical adsorption and partial penetration of protein molecules into the membrane outer monolayer [108]. On the other hand, the fission process can be explained by different types of arguments. Several studies on PLA2 suggest that the enzyme activity is inherently dependent on, and modulated by, the physical state of the substrate. Any event increasing lipid packing disorder, for example, membrane component segregation and domain formation, undergoing phase transitions [97], favors PLA2 incorporation in the bilayer and enzymatic activity. Therefore, this activity on the membrane is likely to be higher at the  $L_o/L_d$  domain interface where LysoPC, which is a product of PLA2 activity, destabilizes the lipid bilayer structure. Indeed, progressive thinning or rupture of the bilayer, decrease of

membrane bending and stretching rigidity, and water permeability increase as well as formation of hydrophilic pores have been observed in the presence of LysoPC [109,110]. Grandbois *et al.* [111] showed, by atomic force microscopy, the membrane heterogeneity (formation of channels (annealing)), which appeared in DPPC supported bilayers as a result of hydrolysis by PLA2. They concluded that there is segregation into intact bilayer, and thinner LysoPC-enriched bilayer. The difference in their thickness was 1.5 nm. On the other hand, using the same technique, Rinia *et al.* [112] studied supported lipid bilayers composed of DOPC/SM/CHOL (45/45/10). They found that the bilayer thickness of the  $L_o$  phase was  $(0.9 \pm 0.1)$  nm larger than the  $L_d$  phase. In our case, PLA2 acts on the  $L_d$  lipid bilayer, around the  $L_o$  domains. Therefore, we may expect that the difference in the thickness between the  $L_o$  phase and the LysoPC-enriched  $L_d$  phase would be at least larger than 1.5 nm, due to accumulation of the two effects. According to our experiments, we demonstrated that a threshold sPLA2 activity is needed to trigger the  $L_o$  domain fission. To show that LysoPC is the key molecule to the fission mechanism, but not other enzymatic products, such as the fatty acid, we treated the  $L_o/L_d$  membranes with LysoPC micelles. Again,  $L_o$  domain fission was observed. Thus, we hypothesized that all molecules characterized by cone-like molecular shape should also induce  $L_o$  domain budding and fission and it was confirmed.

Detergent molecules and LysoPC exhibit a steric and amphiphilic asymmetry in their molecular shape [113,114]. A molecule of this type is characterized by hydrophilic polar head with a cross section  $H$  and hydrophobic part ( $C$ ) that describe the asymmetry of the amphiphilic molecule. In the case where  $H > C$ , the asymmetry is defined as positive. This type of molecule could be schematically presented as inverted cone-like shape. These are therefore expected to stabilize positively curved membrane edges in contact with water and to form pore-like structures.

In cases in which the headgroup and lipid backbone have similar cross-sectional areas  $H \approx C$ , the molecule has a cylindrical shape such as PC. Lipids with a small headgroup  $H < C$  like CHOL and phosphatidylethanolamine are cone shaped.

Bearing in mind such properties, we suggest the following schematic molecular mechanism for raft vesicle expulsion (presented as a sketch in Fig. 7.18). Whatever the origin of molecules with positive steric asymmetry, some of these molecules would accumulate on the  $L_o/L_d$  interface. Inverted cone-shaped molecules can be PLA2-generated LysoPC (Fig. 7.18A and C) in the  $L_d$  phase,  $L_o$  phase stays intact (PLA2 substrate is not available within)

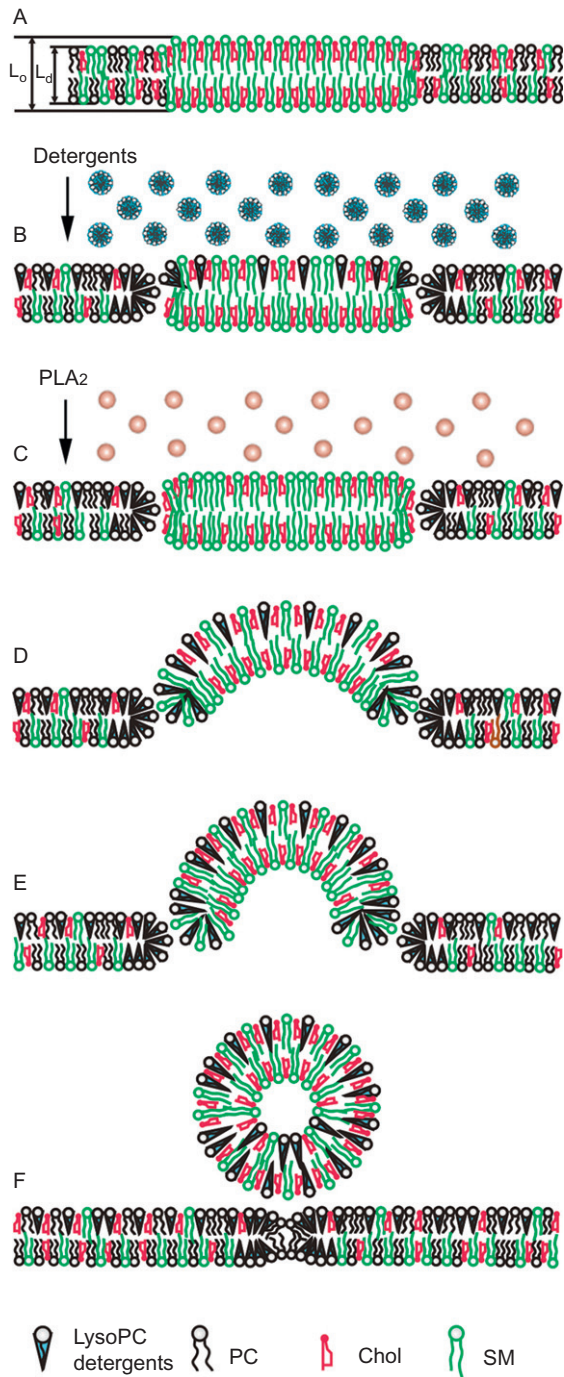


**Figure 7.18** Schematic model of the mechanism of  $L_0$  domain budding and fission from GUV: (A)  $L_0$  domain surrounded by  $L_d$  matrix,  $L_0$  phase thicker than  $L_d$  one; (B) treatment of  $L_0/L_d$  membrane with detergents (natural cell detergent-lysophosphatidylcholine, Triton X-100, and Brij 98) characterizing with inverted cone-shaped molecules; (C) treatment with PLA<sub>2</sub>; (D)  $L_0$  domain budding; (E) budding is able to reach a hemisphere; (F)  $L_0$  domain fission, formation of vesicle only in  $L_0$  phase, closing of parent  $L_d$  vesicle.

or has externally added detergents which partition into two phases (Fig. 7.18A and B). In  $L_o/L_d$  interface, the lipid packing is already broken and the formation of pores would be energetically more favorable. PLA2 adsorption triggers the initial membrane budding at the raft sites. The enzyme activity occurs around the boundary between the raft and the rest of the substrate membrane (Fig. 7.18C). Detergents partition more readily into the  $L_d$  phase than the  $L_o$  one [115] (Fig. 7.18B). It seems that this peculiarity in the detergent experiments is not decisive for the scenario of the  $L_o$  domain budding and fission [103]. The cone-shaped molecules exhibit a slow flip-flop, in the order of several hours [116]. Thus, one may assume that it is mainly distributed in the outer lipid leaflet during the time scale of our experiments. Peterlin *et al.* [117] suggest that regardless of the mechanism of lipid translocation (phospholipid/oleic acid system), flip-flop, or nonspecific convective flow (the latter is caused by the formation of membrane defects or pores), membrane budding is triggered. The accumulation of inverted cone-shaped molecules at the  $L_o/L_d$  interface perturbs lipid packing, leaving space for water molecules to penetrate deeper into the lipid bilayer (Fig. 7.18D). Moreover, the bilayer thickness difference at the raft boundary is increasing in parallel due to the bilayer enrichment of detergent molecules (Triton X-100, Brij 98, and LysoPC) as mentioned. This process leads to an increase of the free energy, and the corresponding line tension, at the raft boundary, which is relaxed by forcing further membrane bending (Fig. 7.18E) raft vesicle formation and fission (Fig. 7.18F).

As suggested above, this process might occur without intensive water flux and mixing between inner and outer aqueous compartments and thereby might represent a proper model for membrane budding and vesicle formation.



## 5. CONCLUSIONS AND BIOLOGICAL IMPLICATIONS

Interest in the SM signaling pathway has increased very rapidly over the last few years. The first step of the SM pathway is the activation of cellular SMase leading to degradation of SM and formation of CER. By using complex biomimetic systems, we showed SMase activity on heterogeneous membrane. The generation of CER does not allow maintaining of the raft-like structures. Gel-like domains appeared instead.

In our studies, we reported that SM acts as an inhibitor of various forms of PLA2 (secretory [100,118] and cytosolic [101]), thus, playing a protective role in maintaining the integrity of cellular membranes, whereas the

products of its degradation, CERs, are powerful activators of these enzymes [119]. Thus, it was suggested that the generated CER segregates into complex nanodomains, which underlie the formation of membrane defects, occurring as a prerequisite for augmentation of enzyme activity. The experiments with model membranes suggest that CER/SM interactions dominate over those of SM/CHOL. Thus, CER sequesters SM, making the GPL substrate more susceptible for the PLA2 hydrolysis. At the cellular level, the events probably follow the same model because a similar behavior is reproduced upon treatment of CHO-2B cells with SMase [101,119]. It is known that the activation of this enzyme, due to different stress factors for example, precedes PLA2 activation. We assume that this intrinsic capacity of CER could make it a potential modulator of PLA2 activity in cells. According to our results, PLA2 activity in heterogeneous membranes induces morphological process such as membrane fragmentation and raft-like budding and fission [47,80,98]. In addition, it was reported that PLA2 is a mediator of membrane shape and function in membrane trafficking [120].

It is supposed that the product of CER hydrolysis, SPH, also modulates the susceptibility of membrane phospholipids to PLA2 [99]. However, it is noteworthy that while studies on SM and CERs and their role in cell biology are quite advanced, very little is currently clear about the biophysical properties of SPH and SPH-1-P, known as second messengers in cell proliferation and survival, and as functional participants in the “CER/SPH-1-P rheostat” [70].

Our research on the miscibility properties of SLs revealed that CER and SPH exhibit a different domain pattern depending on the surrounding lipid matrix [80–82]. In a GPL matrix, they segregate in gel leaf-like domains, whereas CHOL presence increases their miscibility by melting its gel domains in a concentration-dependent manner.

SM stabilizes the gel phase and thus decreases CER miscibility in the presence of CHOL [81]. SM initiates specific CER–SM interactions to form a highly ordered gel phase appearing at temperatures higher than pure CER gel phase in PC matrix. Larger micron-scale  $L_o$  domains were formed in the presence of 10 mol% CER compared to the control raft mixtures [80]. Higher CER concentration leads to the formation of SM–CER gel phase. Thus, less SM participates in the formation of  $L_o$  domains. In its turn, SPH stabilizes the formation of  $L_o$  phase, increasing the temperature of domain formation and thus their fraction.

All these results implied that CER and SPH are also modulators of the lipid phase separation and thus they could exert their biological role, not



only through direct binding to proteins but also indirectly, by influencing their sorting by membranes and thus modulating cell signaling. Very small amounts of CER and SPH are needed to induce cellular response, but the generation of these two molecules by enzyme reactions can reach high local concentrations in membranes. Obviously, a study of the physicochemical properties of all individual elements of the SM signaling pathway (SM, CER, SPH, and SPH-1-P) is crucial for understanding their role in the modulation of various pathological processes in cells and for finding new ways for their control.

Membrane budding is a ubiquitous phenomenon related to biological cell functions representing the initial stage of transport vesicle formation for inter-membrane trafficking of lipids and proteins [121]. The Golgi complex appears to be a central sorting device for the endocytic/exocytic pathways. The biosynthesis of certain important lipid components of rafts, that is, the SLs, takes place in the Golgi complex. The SM-CHOL-based raft domains generated in the Golgi membrane, as well as the proteins inherently coupled to them, might be sorted and trafficked to the plasma membrane by means of membrane fission and transport vesicle formation [122]. On the other hand, it seems that the lipids and proteins constituting the Golgi complex microdomains are efficiently segregated from the COPI-coated vesicles [123]. Rafts appear to be also involved in endocytosis processes and retrograde transport of plasma membrane components to intracellular compartments. The exact nature of the cellular mechanisms involved in the vesicular trafficking of lipid rafts is still a matter of debate [124,125]. In this review, we have presented model experiments and described a possible mechanism for raft vesicle expulsion due to the PLA2 activity. This leads us to the proposal that the presence of active PLA2 in the cell is an important factor for triggering, developing, and finalizing the process of raft-transporting vesicle formation from organelles and plasma membranes. For example, PLA2 might play an important role in the direct transport of rafts from Golgi to plasma membranes by means of trafficking vesicles. The efficiency of this possible direct transport would be of crucial importance for ensuring raft functions in the plasma membrane, as platforms concentrating a large variety of biologically active proteins.

Overall, this review demonstrates the high potential of cell-scale biomimetic systems such as giant vesicles in studying lipid phase separation, how it is dynamically modulated by enzyme activities and what membrane-associated reshape transformations are observed. Many years ago, Aristotle stated that “without image, thinking is impossible.” GUVs together with high technologies in the field of optical microscopy represent a tool by means

of which we can observe and image how the molecules organize in the membranes. Understanding the lipid–lipid, lipid–protein, and protein–protein communications in the two–dimensional membrane plane would provide the key to identify and explain the processes in the third dimension, that is, the communications between different organelles and cells.

## ACKNOWLEDGMENTS

We would like to apologize to all authors who have contributed to the present topic but whose work has not been cited in the review because of the imposed restrictions in volume.

Some of the discussed work of the review's authors cited here were financially supported by the Bulgarian Fund for Scientific Research (DTK 02/5-2009).

## REFERENCES

- [1] S.J. Singer, G.L. Nicolson, The fluid mosaic model of the structure of cell membranes, *Science* 175 (1972) 720–731.
- [2] L.J. Pike, The challenge of lipid rafts, *J. Lipid Res.* 50 (2009) S323–S328.
- [3] B.F. Lilemeier, J.R. Pfeiffer, Z. Surviladze, B.S. Wilson, M.M. Davis, Plasma membrane-associated proteins are clustered into islands attached to the cytoskeleton, *PNAS* 103 (2006) 18992–18997.
- [4] A. Kusumi, C. Nakada, K. Ritchie, K. Murase, K. Suzuki, H. Murakoshi, R.S. Kasai, J. Kondo, T. Fujiwara, Paradigm shift of the plasma membrane concept from the two-dimensional continuum fluid to the partitioned fluid: high-speed single-molecule tracking of membrane molecules, *Annu. Rev. Biophys. Biomol. Struct.* 34 (2005) 351–378.
- [5] K. Simons, M.J. Gerl, Revitalizing membrane rafts: new tools and insights, *Nat. Rev. Mol. Cell Biol.* 11 (2010) 688–699.
- [6] V. Michel, M. Bakovic, Lipid rafts in health and disease, *Biol. Cell* 99 (2007) 129–140.
- [7] K. Simons, E. Ikonen, Functional rafts in cell membranes, *Nature* 387 (1997) 569–572.
- [8] P.E. Bickel, Lipid rafts and insulin signaling, *Am. J. Physiol. Endocrinol. Metab.* 282 (2002) E1–E10.
- [9] J. Pohl, A. Ring, U. Korkmaz, R. Ehehalt, W. Stremmel, FAT/CD36-mediated long-chain fatty acid uptake in adipocytes requires plasma membrane rafts, *Mol. Biol. Cell* 16 (2005) 24–31.
- [10] H. Kamiguchi, The region-specific activities of lipid rafts during axon growth and guidance, *J. Neurochem.* 98 (2006) 330–335.
- [11] R. Willmann, S. Pun, L. Stallmach, G. Sadasivam, A.F. Santos, P. Caroni, C. Fuhrer, Cholesterol and lipid microdomains stabilize the postsynapse at the neuromuscular junction, *EMBO J.* 25 (2006) 4050–4060.
- [12] A. Garsia, X. Cayla, A. Fleischer, J. Guergnon, F.A.–F. Canas, M.P. Rebollo, F. Roncal, A. Rebollo, Rafts: a simple way to control apoptosis by subcellular redistribution, *Biochimie* 85 (2003) 727–731.
- [13] T.S. Soderstrom, S.D. Nyberg, J.E. Eriksson, CD95 capping is ROCK-dependent and dispensable for apoptosis, *J. Cell Sci.* 118 (2005) 2211–2223.
- [14] D. Mandal, A. Mazumder, P. Das, M. Kundu, J. Basu, Fas-, caspase 8-, and caspase 3-dependent signaling regulates the activity of the aminophospholipids translocase and phosphatidylserine externalization in human erythrocytes, *J. Biol. Chem.* 280 (2005) 39460–39467.
- [15] M.D. Jacobson, M. Weil, M.C. Raff, Programmed cell death in animal development, *Cell* 88 (1997) 347–354.

- [16] M.P. Mattson, Apoptosis in neurodegenerative disorders, *Nat. Rev. Mol. Cell Biol.* 1 (2000) 20–29.
- [17] F. Mollinedo, C. Gajate, Fas/CD95 death receptor and lipid rafts: new targets for apoptosis-directed cancer therapy, *Drug Resist. Updat.* 9 (2006) 51–73.
- [18] C. Gajate, F. Gonzales-Camacho, F. Mollinedo, Involvement of rafts aggregates enriched in Fas/CD95 death-inducing signaling complex in the antileukemic action of edelfosine in Jurkat cells, *PLoS One* 4 (2009) e5044–e5055.
- [19] M. Angelova, D. Dimitrov, Liposome electroformation, *Faraday Discuss. Chem. Soc.* 81 (1986) 303–311.
- [20] M. Angelova, S. Soleau, P. Meleard, J.-F. Faucon, P. Bothorel, Preparation of giant vesicles by external AC electric fields: kinetics and applications, *Prog. Colloid Polym. Sci.* 89 (1992) 127–131.
- [21] T. Pott, H. Bouvrais, P. Meleard, Giant unilamellar vesicle formation under physiologically relevant conditions, *Chem. Phys. Lipids* 154 (2008) 115–119.
- [22] J.I. Pavlic, J. Genova, G. Popkirov, V. Kralj-Iglic, A. Iglic, M. Mitov, Mechanoformation of neutral giant phospholipid vesicles in high ionic strength solution, *Chem. Phys. Lipids* 164 (2011) 727–731.
- [23] M. Fidorra, L. Duelund, C. Leidy, A.C. Simonsen, L.A. Bagatolli, Absence of fluid-ordered/fluid-disordered phase coexistence in ceramide/POPC mixtures containing cholesterol, *Biophys. J.* 90 (2006) 4437–4451.
- [24] E.A. Evans, D. Needham, Physical properties of surfactant bilayer membranes: thermal transitions, elasticity, rigidity, cohesion, and colloidal interactions, *J. Phys. Chem. B* 91 (1987) 4219–4228.
- [25] H.G. Dobreiner, J. Kas, D. Noppl, I. Sprenger, E. Sackmann, Budding and fission of vesicles, *Biophys. J.* 65 (1993) 1396–1403.
- [26] D. Needham, R.S. Nunn, Elastic deformation and failure of lipid bilayer membranes containing cholesterol, *Biophys. J.* 58 (1990) 997–1009.
- [27] P. Meleard, C. Gerbeaud, T. Pott, L. Fernandez-Puente, I. Bivas, M.D. Mitov, J. Dufourcq, P. Bothorel, Bending elasticities of model membranes: influences of temperature and sterol content, *Biophys. J.* 72 (1997) 2616–2629.
- [28] L.-R. Montes, A. Alonso, F.M. Goni, L.A. Bagatolli, Giant unilamellar vesicles electroformed from native membranes and organic lipid mixtures under physiological conditions, *Biophys. J.* 93 (2007) 3548–3554.
- [29] K. Akashi, H. Miyata, H. Itoh, K. Kinoshita Jr., Preparation of giant liposomes in physiological conditions and their characterization under an optical microscope, *Biophys. J.* 71 (1996) 3242–3250.
- [30] G. Staneva, M. Seigneuret, H. Conjeaud, N. Puff, M.I. Angelova, Making a tool of an artifact: the application of photoinduced Lo domains in giant unilamellar vesicles to the study of Lo/Ld phase spinodal decomposition and its modulation by the ganglioside GM1, *Langmuir* 27 (2011) 15074–15082.
- [31] C. Dietrich, L.A. Bagatolli, Z.N. Volovyk, N.L. Tompson, M. Levi, K. Jacobson, E. Gratton, Lipid rafts reconstituted in model membranes, *Biophys. J.* 80 (2001) 1417–1428.
- [32] S.L. Veatch, S.L. Keller, Separation of liquid phases in giant vesicles of ternary mixtures of phospholipids and cholesterol, *Biophys. J.* 85 (2003) 3074–3083.
- [33] L.A. Bagatolli, E. Gratton, A correlation between lipid domain shape and binary phospholipid mixture composition in free standing bilayers: a two-photon fluorescence microscopy study, *Biophys. J.* 79 (2000) 434–447.
- [34] G. Staneva, C. Chachaty, C. Wolf, P. Quinn, Comparison of liquid-ordered bilayer phases containing cholesterol or 7-dehydrocholesterol in modeling Smith-Lemli-Opitz syndrome, *J. Lipid Res.* 51 (2010) 1810–1822.

- [35] A.J. Garcia-Saez, S. Chiantia, P. Schwille, Effect of line tension on the lateral organization of lipid membranes, *J. Biol. Chem.* 282 (2007) 33537–33544.
- [36] M.I. Angelova, I. Tsoneva, Interactions of DNA with giant liposomes, *Chem. Phys. Lipids* 101 (1999) 123–137.
- [37] T. Baumgart, A.T. Hammond, P. Sengupta, S.T. Hess, D. Holowka, B. Baird, W.W. Webb, Large-scale fluid/fluid phase separation of proteins and lipids in giant plasma membrane vesicles, *PNAS* 104 (2007) 3165–3170.
- [38] E. Sezgin, H.J. Kaiser, T. Baumgart, P. Schwille, K. Simons, L. Levental, Elucidating membrane structure and protein behavior using giant plasma membrane vesicles, *Nat. Protoc.* 7 (2012) 1042–1051.
- [39] A. Varnier, F. Kermarrec, I. Blesneac, C. Moreau, L. Liguori, J.L. Lenormand, N. Picollet-D’ahan, A simple method form the reconstitution of membrane proteins into giant unilamellar vesicles, *J. Membr. Biol.* 233 (2010) 85–92.
- [40] N. Khalifat, N. Puff, M. Dliia, M.I. Angelova, Amyloid-beta and the failure to form mitochondrial cristae: a biomimetic study involving artificial membranes, *J. Alzheimers Dis.* 28 (2012) 33–48.
- [41] K. Bacia, C.G. Schuette, N. Kahya, R. Jahn, P. Schwille, SNAREs prefer liquid-disordered over “raft”-(liquid-ordered) domains when reconstituted into giant unilamellar vesicles, *J. Biol. Chem.* 279 (2004) 37951–37955.
- [42] H.-J. Kaiser, D. Lingwood, I. Levental, J.L. Sampaio, L. Kalvodova, L. Rajendran, K. Simons, Order of lipid phases in model and plasma membranes, *PNAS* 106 (2009) 16645–16650.
- [43] R. Wick, M.I. Angelova, P. Walde, P.L. Luisi, Microinjection into giant vesicles and light microscopy investigation of enzyme-mediated vesicle transformations, *Chem. Biol.* 3 (1996) 105–111.
- [44] J.M. Holopainen, M. Subramanian, P.K.J. Kinnunen, Sphingomyelinase induces lipid microdomains formation in fluid phosphatidylcholine/sphingomyelin membrane, *Biochemistry* 37 (1998) 17562–17570.
- [45] J.M. Holopainen, M. Angelova, P.K.J. Kinnunen, Vectorial budding of vesicles by asymmetrical enzymatic formation of ceramide in giant liposomes, *Biophys. J.* 78 (2000) 830–838.
- [46] S.A. Sanchez, L.A. Bagatolli, E. Gratton, T.L. Hazlett, A two-photon view of an enzyme at work: *Crotalus atrox* venom PLA2. Interaction with single-lipid and mixed-lipid giant unilamellar vesicles, *Biophys. J.* 82 (2002) 2232–2243.
- [47] G. Staneva, M.I. Angelova, K. Koumanov, Phospholipase A2 promotes raft budding and fission from giant liposomes, *Chem. Phys. Lipids* 129 (2004) 53–62.
- [48] T.M. Konyakhina, S.L. Goh, J. Amazon, F.A. Heberle, J. Wu, G.W. Feigenson, Control of a nanoscopic-to-macroscopic transition: modulated phases in four-component DSPC/DOPC/POPC/Chol giant unilamellar vesicles, *Biophys. J.* 101 (2011) L08–L10.
- [49] S.L. Veatch, I.V. Polozov, K. Gawrisch, S.L. Keller, Liquid domains in vesicles investigated by NMR and fluorescence microscopy, *Biophys. J.* 86 (2004) 2910–2922.
- [50] S.L. Veatch, S.L. Keller, Seeing spots: complex phase behavior in simple mixtures, *Biochim. Biophys. Acta* 1746 (2005) 172–185.
- [51] J. Kolrach, P. Schwille, W.W. Webb, G.W. Feigenson, Characterization of lipid bilayer phases by confocal microscopy and fluorescence correlation spectroscopy, *PNAS* 96 (1999) 8461–8466.
- [52] T. Baumgart, S.T. Hess, W.W. Webb, Imaging coexisting fluid domains in biomembrane models coupling curvature and line tension, *Nature* 425 (2003) 821–824.
- [53] F.M. Menger, J.S. Keiper, Chemistry and physics of giant vesicles as biomembrane models, *Curr. Opin. Chem. Biol.* 2 (1998) 726–732.

- [54] A. Roux, G. Cappello, J. Cartaud, J. Prost, B. Goud, P. Bassereau, A minimal system allowing tubulation with molecular motors pulling on giant liposomes, *PNAS* 99 (2002) 5394–5399.
- [55] G. Staneva, T. Lupanova, C. Chachaty, D. Petkova, K. Koumanov, R. Pankov, A. Momchilova, Structural organization of plasma membrane lipids isolated from cells cultured as a monolayer and in tissue-like conditions, *J. Colloid Interface Sci.* 359 (2011) 202–209.
- [56] M. Fidorra, A. Garcia, J.H. Ipsen, S. Hartel, L.A. Bagatolli, Lipid domains in giant unilamellar vesicles and their correspondence with equilibrium thermodynamic phases: a quantitative fluorescence microscopy imaging approach, *Biochim. Biophys. Acta* 1788 (2009) 2142–2149.
- [57] G.W. Feigenson, Phase behaviour of lipid mixtures, *Nat. Chem. Biol.* 2 (2006) 560–563.
- [58] G.W. Feigenson, J.T. Buboltz, Ternary phase diagram of dipalmitoyl-PC/dilauroyl-PC/cholesterol: nanoscopic domain formation driven by cholesterol, *Biophys. J.* 80 (2001) 2775–2788.
- [59] J. Zhao, J. Wu, H. Shao, F. Kong, N. Jain, G. Hunt, G. Feigenson, Phase studies of model biomembranes: macroscopic coexistence of La + Lb, with light-induced coexistence of La + Lo phases, *Biochim. Biophys. Acta* 1768 (2007) 2777–2786.
- [60] S.L. Veatch, S.L. Keller, Organization in lipid membranes containing cholesterol, *Phys. Rev. Lett.* 89 (2002) 268101.
- [61] K. Bacia, P. Schwille, T. Kurzchalia, Sterol structure determines the separation of phases and the curvature of the liquid-ordered phase in model membranes, *PNAS* 102 (2005) 3272–3277.
- [62] M.E. Beattie, S.L. Veatch, B.L. Stottrup, S.L. Keller, Sterol structure determines miscibility versus melting transitions in lipid vesicles, *Biophys. J.* 89 (2005) 1760–1768.
- [63] S.L. Veatch, O. Soubias, S.L. Keller, K. Gawrisch, Critical fluctuations in domain-forming lipid mixtures, *PNAS* 104 (2007) 17650–17655.
- [64] A.G. Ayuyan, F.S. Cohen, Lipid peroxides promote large rafts: effects of excitation of probes in fluorescence microscopy and electrochemical reactions during vesicle formation, *Biophys. J.* 91 (2006) 2172–2183.
- [65] M. Sud, E. Fahy, D. Cotter, A. Brown, E. Dennis, C. Glass, R. Murphy, C. Raetz, D. Russell, S. Subramaniam, LMSD: LIPID MAPS structure database, *Nucleic Acids Res.* 35 (2006) D527–D532.
- [66] R. Koynova, M. Caffrey, Phases and phase transition of the sphingolipids, *Biochim. Biophys. Acta* 1255 (1995) 213–236.
- [67] M. Masserini, D. Ravasi, Role of sphingolipids in the biogenesis of membrane domains, *Biochim. Biophys. Acta* 1532 (2001) 149–161.
- [68] E. Gulbins, S. Dreschers, B. Wilker, H. Grassme, Ceramide, membrane rafts and infections, *J. Mol. Med.* 82 (2004) 357–363.
- [69] T.A. Taha, T.D. Mullen, L.M. Obeid, A house divided: ceramide, sphingosine, and sphingosine-1-phosphate in programmed cell death, *Biochim. Biophys. Acta* 1758 (2006) 2027–2036.
- [70] O. Cuvillier, Sphingosine in apoptosis signaling, *Biochim. Biophys. Acta* 1585 (2002) 153–162.
- [71] E.L. Laviad, L. Albee, I. Pankova-Kholmyansky, S. Epstein, H. Park, A.H. Merrill, A.H. Futerman, Characterization of ceramide synthase 2-tissue distribution, substrate specificity, and inhibition by sphingosine 1-phosphate, *J. Biol. Chem.* 283 (2008) 5677–5684.
- [72] T. Levade, J.P. Jaffrezou, Signalling sphingomyelinases: which, where, how and why? *Biochim. Biophys. Acta* 1483 (1999) 1–17.

- [73] R.J. Veldman, N. Maestre, O.M. Aduib, J.A. Medin, R. Salvayre, T. Levade, A neutral sphingomyelinase resides in sphingolipid-enriched microdomains and is inhibited by the caveolin-scaffolding domain: potential implications in tumour necrosis factor signalling, *Biochem. J.* 355 (2001) 859–868.
- [74] A. Cremesti, F. Paris, H. Grassme, N. Holler, J. Tschopp, Z. Fuks, E. Gulbins, R. Kolesnick, Ceramide enables Fas to cap and kill, *J. Biol. Chem.* 276 (2001) 23954–23961.
- [75] C. Michel, G. van-Echten-Deckert, J. Rother, K. Sandhoff, E. Wang, Characterization of ceramide synthesis. A dihydroceramide desaturase introduces the 4,5-trans-double bond of sphingosine at the level of dihydroceramide, *J. Biol. Chem.* 272 (1997) 22432–22437.
- [76] M. Tani, M. Ito, Y. Igarashi, Ceramide/sphingosine/sphingosine 1-phosphate metabolism on the cell surface and in the extracellular space, *Cell. Signal.* 19 (2007) 229–237.
- [77] A. Olivera, S. Spiegel, Sphingosine-1-phosphate as 2nd messenger in cell-proliferation induced by Pdgf and Fcs mitogens, *Nature* 365 (1993) 557–560.
- [78] N. Auge, M. Nikolova-Karakashian, S. Carpentier, S. Parthasarathy, A. Negre-Salvayre, R. Salvayre, A.H. Merrill Jr., T. Levade, Role of sphingosine 1-phosphate in the mitogenesis induced by oxidized low density lipoprotein in smooth muscle cells via activation of sphingomyelinase, ceramidase, and sphingosine kinase, *J. Biol. Chem.* 274 (1999) 21533–21538.
- [79] J.A. Hengst, J.M. Guilford, T.E. Fox, X. Wang, E.J. Conroy, J.K. Yun, Sphingosine kinase 1 localized to the plasma membrane lipid raft microdomain overcomes serum deprivation induced growth inhibition, *Arch. Biochem. Biophys.* 492 (2009) 62–73.
- [80] G. Staneva, A. Momchilova, C. Wolf, P.J. Quinn, K. Koumanov, Membrane microdomains: role of ceramides in the maintenance of their structure and functions, *Biochim. Biophys. Acta* 1788 (2009) 666–675.
- [81] G. Staneva, C. Chachaty, C. Wolf, K. Koumanov, P.J. Quinn, The role of sphingomyelin in regulating phase coexistence in complex lipid model membranes: competition between ceramide and cholesterol, *Biochim. Biophys. Acta* 1778 (2008) 2727–2739.
- [82] R. Georgieva, K. Koumanov, A. Momchilova, C. Tessier, G. Staneva, Effect of sphingosine on domain morphology in giant vesicles, *J. Colloid Interface Sci.* 350 (2010) 502–510.
- [83] H.M. McConnel, Harmonic shape transitions in lipid monolayer domains, *J. Phys. Chem.* 94 (1990) 4728–4731.
- [84] S. Hartel, M.L. Fanani, B. Maggio, Shape transitions and lattice structuring of ceramide-enriched domains generated by sphingomyelinase in lipid monolayers, *Biophys. J.* 88 (2005) 287–304.
- [85] N. Garmy, N. Taïeb, N. Yahi, J. Fantini, Interaction of cholesterol with sphingosine: physicochemical characterization and impact on intestinal adsorption, *J. Lipid Res.* 46 (2005) 36–45.
- [86] Megha, E. London, Ceramide selectively displaces cholesterol from ordered lipid domains (rafts): implications for lipid raft structure and function, *J. Biol. Chem.* 279 (2004) 9997–10004.
- [87] S. Chiantia, N. Kahya, J. Ries, P. Schwill, Effects of ceramide on liquid-ordered domains investigated by simultaneous AFM and FCS, *Biophys. J.* 90 (2006) 4500–4508.
- [88] S.M.K. Alanko, K.K. Halling, S. Maunula, J.P. Slotte, B. Ramstedt, Displacement of sterols from sterol/sphingomyelin domains in fluid bilayer membranes by competing molecules, *Biochim. Biophys. Acta* 1715 (2005) 111–121.
- [89] S. Mathias, R. Kolesnick, Ceramide: a novel second messenger, *Adv. Lipid Res.* 25 (1993) 65–90.

- [90] M.L. Fanani, S. Hartel, R. Oliveira, B. Maggio, Bidirectional control of sphingomyelinase activity and surface topography in lipid monolayers, *Biophys. J.* 83 (2002) 3416–3424.
- [91] Y. Taniguchi, T. Ohba, H. Miyata, K. Ohki, Rapid phase change of lipid microdomains in giant vesicles induced by conversion of sphingomyelin to ceramide, *Biochim. Biophys. Acta* 1758 (2006) 145–153.
- [92] J. Bai, R.E. Pagano, Measurement of spontaneous transfer and transbilayer movement of BODIPY-labeled lipids in lipid vesicles, *Biochemistry* 36 (1997) 8840–8848.
- [93] I. Lopez-Montero, N. Rodriguez, S. Cribier, A. Rohl, M. Velez, P.F. Devaux, Rapid transbilayer movement of ceramides in phospholipid vesicles and human erythrocytes, *J. Biol. Chem.* 280 (2005) 25811–25819.
- [94] I. Lopez-Montero, M. Velez, P.F. Devaux, Surface tension induced by sphingomyelin to ceramide conversion in lipid membranes, *Biochim. Biophys. Acta* 1768 (2007) 553–561.
- [95] M. Ibarguren, D.J. Lopez, L.-R. Montes, J. Sot, A.I. Vasil, M.L. Vasil, F.M. Goni, A. Alonso, Imaging the early stages of phospholipase C/sphingomyelinase activity on vesicles containing coexisting ordered-disordered and gel-fluid domains, *J. Lipid Res.* 52 (2011) 635–645.
- [96] R.P. Stock, J. Brewer, K. Wagner, B. Ramos-Cerrillo, L. Duelund, K.D. Jernshoj, L.F. Olsen, L.A. Bagatolli, Sphingomyelinase D activity in model membranes: structural effects of in situ generation of ceramide-1-phosphate, *PLoS One* 7 (2012) e36003.
- [97] K. Jorgensen, J. Davidsen, O. Mouritsen, Biophysical mechanism of phospholipase A2 activation and their use in liposome-based drug delivery, *FEBS Lett.* 531 (2002) 23–27.
- [98] G. Staneva, A. Momchilova, M. Angelova, K. Koumanov, Regulatory effect of sphingolipids on secretory phospholipase A2. Comparative study using SUV and GUV, *C. R. Acad. Bulg. Sci.* 57 (2004) 59–64.
- [99] J.W. Huang, E.M. Goldberg, R. Zidovetzki, Ceramide reduces structural defects in phosphatidylcholine bilayers and activates phospholipase A2, *Biochem. Biophys. Res. Commun.* 220 (1996) 834–838.
- [100] K.S. Koumanov, P.J. Quinn, G. Bereziat, C. Wolf, Cholesterol relieves the inhibitory effect of sphingomyelin on type II secretory phospholipase A2, *Biochem. J.* 336 (1998) 625–630.
- [101] E. Klapisz, J. Masliah, G. Bereziat, C. Wolf, K.S. Koumanov, Sphingolipids and cholesterol modulate membrane susceptibility to cytosolic phospholipase A2, *J. Lipid Res.* 41 (2000) 1680–1688.
- [102] D.V. Zhelev, Material property characteristics for lipid bilayers containing lysolipid, *Biophys. J.* 75 (1998) 321–330.
- [103] G. Staneva, M. Seigneuret, K. Koumanov, G. Trugnan, M.I. Angelova, Detergents induce raft-like domains budding and fission from giant unilamellar heterogeneous vesicles. A direct microscopy observation, *Chem. Phys. Lipids* 136 (2005) 55–66.
- [104] P. Drevot, C. Langlet, X.-J. Guo, A.-M. Bernard, O. Colard, J.-P. Chauvin, R. Lasserre, H.-T. He, TCR signal initiation machinery is pre-assembled and activated in a subset of membrane rafts, *EMBO J.* 21 (2002) 1899–1908.
- [105] J.L. Pike, Lipid rafts: heterogeneity on the high seas, *Biochem. J.* 378 (2004) 281–292.
- [106] R. Lipowsky, Domains and rafts in membranes—hidden dimensions of selforganization, *J. Biol. Phys.* 28 (2002) 195–210.
- [107] P.I. Kuzmin, S.A. Akimov, Y.A. Chizmadzhev, J. Zimmerberg, F.S. Cohen, Line tension and interaction energies of membrane rafts calculated from lipid splay and tilt, *Biophys. J.* 88 (2005) 1120–1133.
- [108] J.-M. Allain, M. Ben Amar, Bi-phasic vesicle: instability induced by adsorption of proteins, *Phys. A* 337 (2004) 531–545.

- [109] C. van Echteld, B. de Kruijff, J. Mandersloot, J. Gier, Effects of lysophosphatidylcholines on phosphatidylcholine and phosphatidylcholine/cholesterol liposomes systems as revealed by  $^{31}\text{P}$ -NMR, electron microscopy and permeability studies, *Biochim. Biophys. Acta* 649 (1981) 211–220.
- [110] D. Needham, D.V. Zhelev, Lysolipid exchange with lipid vesicle membranes, *Ann. Biomed. Eng.* 23 (1995) 287–298.
- [111] M. Grandbois, H. Clausen-Schaumann, H. Gaub, Atomic force microscope imaging of phospholipid bilayer degradation by phospholipase A2, *Biophys. J.* 74 (1998) 2398–2404.
- [112] H. Rinia, M. Snel, J. van der Eerden, B. de Kruijff, Visualizing detergent resistant domains and model membranes with atomic force microscopy, *FEBS Lett.* 501 (2001) 92–96.
- [113] P.R. Cullis, B. de Kruijff, Lipid polymorphism and the functional roles of lipids in biological membranes, *Biochim. Biophys. Acta* 559 (1979) 399–420.
- [114] H. Sprong, P. van der Sluijs, G. van Meer, How proteins move lipids and lipids move proteins, *Nat. Rev. Mol. Cell. Biol.* 2 (2001) 504–513.
- [115] H. Heerklotz, Triton promotes domain formation in lipid raft mixtures, *Biophys. J.* 83 (2002) 2693–2701.
- [116] S.P. Bhamidipati, J.A. Hamilton, Interactions of lyso 1-palmitoylphosphatidylcholine with phospholipids: a  $^{13}\text{C}$  and  $^{31}\text{P}$  NMR study, *Biochemistry* 34 (1995) 5666–5677.
- [117] P. Peterlin, V. Arrigler, K. Kogej, A. Svetina, P. Walde, Growth and shape transformations of giant phospholipid vesicles upon interaction with an aqueous oleic acid suspension, *Chem. Phys. Lipids* 159 (2009) 67–76.
- [118] K. Koumanov, C. Wolf, G. Bereziat, Modulation of human type II secretory phospholipase A2 by sphingomyelin and annexin VI, *Biochem. J.* 326 (1997) 227–233.
- [119] K.S. Koumanov, A.B. Momchilova, P.J. Quinn, C. Wolf, Ceramides increase the activity of the secretory phospholipase A2 and alter its fatty acid specificity, *Biochem. J.* 363 (2002) 45–51.
- [120] W.J. Brown, K. Chambers, A. Doody, Phospholipase A2 (PLA2) enzymes in membrane trafficking: mediators of membrane shape and function, *Traffic* 4 (2003) 214–221.
- [121] M. Muniz, M. Martin, J. Hidalgo, A. Velasco, Protein kinase A activity is required for the budding of constitutive transport vesicles from the trans-Golgi network, *PNAS* 94 (1997) 14461–14466.
- [122] R. Pagano, Lipid traffic in eukaryotic cells: mechanism for intracellular transport and organelle-specific enrichment of lipids, *Curr. Opin. Cell Biol.* 2 (1990) 652–663.
- [123] B. Brugger, R. Sandhoff, S. Wegehingel, K. Gorgas, J. Malsam, J. Helms, W. Lehmann, F. Wieland, Evidence for segregation of sphingomyelin and cholesterol during formation of COPI-coated vesicles, *J. Cell Biol.* 151 (2000) 507–517.
- [124] F. van der Goot, J. Gruenberg, Oiling the wheels of the endocytic pathway, *Trends Cell Biol.* 12 (2002) 296–299.
- [125] E. Ikonen, Roles of lipid rafts in membrane transport, *Curr. Opin. Cell Biol.* 13 (2001) 470–477.